

การตรวจวัดเชิงสีของไซยาไนด์ไอออนโดยการเกิดสารประกอบเชิงซ้อนและซิลิกาเคลือบผิวด้วยซีแทบ



บทคัดย่อและแฟ้มข้อมูลฉบับเต็มของวิทยานิพนธ์ตั้งแต่ปีการศึกษา 2554 ที่ให้บริการในคลังปัญญาจุฬาฯ (CUIR)
เป็นแฟ้มข้อมูลของนิสิตเจ้าของวิทยานิพนธ์ ที่ส่งผ่านทางบัณฑิตวิทยาลัย

The abstract and full text of theses from the academic year 2011 in Chulalongkorn University Intellectual Repository (CUIR)
are the thesis authors' files submitted through the University Graduate School.

วิทยานิพนธ์นี้เป็นส่วนหนึ่งของการศึกษาตามหลักสูตรปริญญาวิทยาศาสตรมหาบัณฑิต
สาขาวิชาเคมี ภาควิชาเคมี
คณะวิทยาศาสตร์ จุฬาลงกรณ์มหาวิทยาลัย
ปีการศึกษา 2560
ลิขสิทธิ์ของจุฬาลงกรณ์มหาวิทยาลัย



จุฬาลงกรณ์มหาวิทยาลัย
CHULALONGKORN UNIVERSITY

COLORIMETRIC DETECTION OF CYANIDE IONS USING COMPLEX FORMATION AND
CTAB-COATED SILICA



A Thesis Submitted in Partial Fulfillment of the Requirements
for the Degree of Master of Science Program in Chemistry

Department of Chemistry

Faculty of Science

Chulalongkorn University

Academic Year 2017

Copyright of Chulalongkorn University



จุฬาลงกรณ์มหาวิทยาลัย
CHULALONGKORN UNIVERSITY

ปติตดา สาลี : การตรวจวัดเชิงสีของไซยาไนด์ไอออนโดยการเกิดสารประกอบเชิงซ้อนและ
 ซิลิกาเคลือบผิวด้วยซีแทบ (COLORIMETRIC DETECTION OF CYANIDE IONS USING
 COMPLEX FORMATION AND CTAB-COATED SILICA) อ.ที่ปริกษาวิทยานิพนธ์หลัก:
 ผศ. ดร.เฟื่องฟ้า อุ่นอบ, หน้า.

งานวิจัยชิ้นนี้นำเสนอเทคนิคใหม่สำหรับการตรวจวัดไซยาไนด์ไอออนในสารละลายและน้ำ
 ตัวอย่างด้วยการสังเกตสีของสารประกอบ dicyano-bis-(1,10-phenanthroline)-iron(II) บนผิวของ
 ซิลิกาเคลือบผิวด้วย CTAB โดยสารประกอบเชิงซ้อนดังกล่าวเกิดจากปฏิกิริยาระหว่าง tris(1,10-
 phenanthroline)-iron(II) (เฟอโรอิน) กับ ไซยาไนด์ไอออนในสารละลายที่มีส่วนประกอบของ
 สารละลาย CTAB, โซเดียมไนเตรท ที่พีเอช 10 โดยใช้ฟอสเฟตบัฟเฟอร์ จากนั้นทำการสกัด
 สารประกอบเชิงซ้อนด้วยซิลิกาเคลือบผิวด้วย CTAB ทำให้สีของวัสดุเปลี่ยนจากสีเหลืองอ่อนเป็น
 สีม่วง โดยขึ้นกับความเข้มข้นของไซยาไนด์ไอออนในสารละลาย โดยสามารถสังเกตสีของสารประกอบ
 บนผิวของวัสดุได้ด้วยตาเปล่า ความเข้มสีของวัสดุหลังทำการสกัดสารประกอบสามารถวิเคราะห์ได้
 ด้วยโปรแกรม image J ได้ทำการศึกษาผลของตัวแปร ได้แก่ ความเข้มข้นของเฟอโรอินที่ใช้ในการ
 เกิดสารประกอบ ปริมาตรของสารละลายตัวอย่าง ความเข้มข้นของ CTAB ที่ใช้ในขั้นตอนการเกิด
 สารประกอบ เวลาในการสกัด และ ความเข้มข้นของเฟอโรอินที่ใช้ในการเกิดสารประกอบใน
 สารละลายผสมที่มี CTAB นอกจากนี้ยังได้ศึกษาผลกระทบของเมทริกซ์ในน้ำและผลของแอนไอออน
 ต่างๆ โดยพบว่าเมทริกซ์ของน้ำส่งผลต่อการวิเคราะห์ไซยาไนด์ในน้ำด้วยวิธีของการวิจัยนี้ ผลการ
 ทดลองแสดงความสัมพันธ์เชิงเส้นตรงในช่วงความเข้มข้นของไซยาไนด์ 30-150 ไมโครโมลาร์ ให้
 ขีดจำกัดของการตรวจวัดอยู่ที่ 17.2 ไมโครโมลาร์ และผลจากการทดลองพบว่าค่าร้อยละการได้
 กลับคืนของไซยาไนด์จากน้ำตัวอย่าง (%recovery) อยู่ในช่วง 83.00-99.49 % และค่าความเที่ยงใน
 การวิเคราะห์ (%RSD) อยู่ในช่วง 1.23-7.14% โดยเทคนิคที่นำเสนอนี้สามารถประยุกต์ในการ
 ตรวจวัดไซยาไนด์ในน้ำตัวอย่างด้วยความแม่นยำและความเที่ยงที่ยอมรับได้

ภาควิชา เคมี ปลายมือเขียนิสิต

สาขาวิชา เคมี ปลายมือชื่อ อ.ที่ปริกษาหลัก

ปีการศึกษา 2560

5871982023 : MAJOR CHEMISTRY

KEYWORDS: CYANIDE, SILICA GEL, COLORIMETRIC DETECTION, CTAB-COATED SILICA

PATITA SALEE: COLORIMETRIC DETECTION OF CYANIDE IONS USING COMPLEX FORMATION AND CTAB-COATED SILICA. ADVISOR: ASST. PROF. FUANGFA UNOB, Ph.D., pp.

This research presents a new colorimetric method of cyanide detection in solution and water samples based on the extraction of dicyano-bis-(1,10-phenanthroline)-iron(II) complex onto CTAB-coated silica. The complex was formed at pH 10 by using phosphate buffer via the complex formation between tris-(1,10-phenanthroline)-Iron(II) (ferroin) with cyanide ions in CTAB media. When the complex was extracted onto CTAB-coated silica, it resulted in a color change of the material from pale yellow to purple. The changing of color corresponded to cyanide concentration which could be observed by naked-eyes and the color intensity was determined by Image J. The effects of various parameters were investigated including ferroin concentration used to form complex, sample volume, CTAB concentration in complex formation step, extraction time and ferroin concentration used to form complex in CTAB media. Moreover, the effect of water sample matrix and foreign anions were also studied. This method had a linear range from 30-150 mM and limit of detection ($S/N=3$) of 17.2 mM. The recovery of cyanide in sample observed by the proposed method was 83.00-99.49% and standard deviation was 1.23-7.14%. This method was applied to determine cyanide in water samples with acceptable accuracy and precision.

Department: Chemistry

Student's Signature

Field of Study: Chemistry

Advisor's Signature

Academic Year: 2017

ACKNOWLEDGEMENTS

First of all, this thesis would not be possible without my advisor, I really would like to give special thanks to my thesis advisor, Assistant Professor Dr. Fuangfa Unob for precious suggestions, kind assisting and supports, encouragement and valuable time. I really appreciate her dedication to my thesis and also other students. I have learned so many things from her not only scientific knowledge but also life management. In addition, I would like to thank Associate Professor Dr. Vudhichai Parasuk, Assistant Professor Dr. Boosayarat Tomapatanaget from the department of chemistry, Chulalongkorn University and Associate Professor Dr. Atitaya Siripinyanond from the department of chemistry, Mahidol University for their kinds suggestions and comments as a committee member. Moreover, I would like to thank Petromat, the Center of Excellence on Petrochemical and Materials Technology for financial support.

I really appreciate all supports, suggestions, and useful discussion from the members of Environment Analysis Research Unit (EARU) that also help to improve my work and encourage me for working in the lab. Also, I am very thankful for all kind help, friendship from my friends.

Last, I am very grateful to my family for their love, kind support and encouragement throughout my study and Professor Dr. Kate Grudpan for supporting me to have special experience internship at the Institute for Nuclear Waste Disposal, Karlsruhe institute of technology, Germany. I would not have completed this thesis without all the supports that I received from everyone of them.

CONTENTS

	Page
THAI ABSTRACT	iv
ENGLISH ABSTRACT	v
ACKNOWLEDGEMENTS	vi
CONTENTS	vii
LIST OF TABLES	x
LIST OF FIGURES	xi
LIST OF SCHEMES	xiii
LIST OF ABBREVIATIONS	xiv
CHAPTER I INTRODUCTION.....	1
1.1 Statement of background and problem	1
1.2 Research objective	2
1.3 Scope of the research.....	3
1.4 The benefit of this research	3
CHAPTER II THEORY AND LITERATURE REVIEW	4
2.1 Cyanide	4
2.2 Methods for cyanide detection	6
2.2.1 Electrochemical methods.....	6
2.2.2 Ion chromatography.....	8
2.3 Colorimetry and spectrophotometry.....	10
2.4 Modification of silica with CTAB.....	14
2.5 Quantitative analysis using value color space	16
3.1 Chemicals	17

	Page
3.2 Instruments	18
3.3 Preparation and characterization of CTAB-coated silica.....	18
3.3.1 Preparation of CTAB-coated silica.....	18
3.3.2 Characterization of CTAB-coated silica	19
3.4 Preparation of ferroin reagent.....	19
3.5 Colorimetric determination of cyanide	19
3.5.1 Cyanide detection	19
3.5.2 Optimization of cyanide determination method.....	20
3.6 Method performance.....	21
3.6.1 Linear working range.....	21
3.6.2 Limit of detection.....	21
3.7 Effect of foreign ions	22
3.8 Determination of cyanide in water samples	22
3.8.1 Effect of water sample matrix	22
3.8.2 Accuracy and precision in water sample analysis	23
CHAPTER IV RESULTS AND DISCUSSIONS.....	26
4.1 Material characterization.....	27
4.1.1 Characterization of CTAB-coated silica	27
4.1.2 Characterization of complexes.....	29
4.2 Colorimetric detection of cyanide	31
4.2.1 Effect of ferroin concentration	32
4.2.2 Effect of sample volume	34
4.2.3 Effect of CTAB concentration used in complex formation step.....	36

	Page
4.2.4 Extraction time.....	39
4.2.5 Effect of ferriin concentration used in complex formation in CTAB- containing media	42
4.3 Method performance.....	44
4.3.1 linear working range	44
4.3.2 Limit of detection.....	45
4.4 Effect of foreign ions	46
4.5 Determination of cyanide in water samples.....	48
4.5.1 Effect of water sample matrix	48
4.5.2 Accuracy and precision in water sample analysis	50
CHEAPTER V CONCLUSION.....	53
5.1 Conclusion.....	53
5.2 Suggestion for future work.....	54
.....	55
REFERENCES	55
VITA.....	62

LIST OF TABLES

	page
Table 3.1 List of chemicals.....	17
Table 3.2 List of instruments	18
Table 3.3 The range of values of studied parameters for cyanide detection	20
Table 3.4 Percent recovery and percent RSD of analytical results obtained at different analyte concentrations according to AOAC international.....	24
Table 3.5 List of conditions of ion chromatography method	25
Table 3.6 Details of camera condition.....	25
Table 4.1 Effect of ferroin concentration on the color of the material used in the detection of cyanide in a concentration range of 0-120 μM	33
Table 4.2 Effect of sample volume on the color of the material used in the detection of cyanide in a concentration range of 0-120 μM	35
Table 4.3 Effect of CTAB concentration added during complex formation step on the color of silica gel and CTAB-coated silica used in the detection of cyanide	37
Table 4.4 Effect of extraction time used on the color of material used in the detection of cyanide in a concentration 0, 50 and 100 μM	40
Table 4.5 Effect of ferroin concentration used in complex formation in CTAB- containing media on the color of material used in the cyanide detection in a concentration range of 0-150 μM	43
Table 4.6 Effect of foreign ions on material color used to detect cyanide ions	47
Table 4.7 Determination of cyanide in water samples by the proposed method and ion chromatography method	52

LIST OF FIGURES

	page
Figure 2.1 Cyanogenic glycosides in plants.	5
Figure 2.2 Process of cyanide metabolism in living organism.	6
Figure 2.3 Chromatogram of cyanate (1 ppm) and other anions.	8
Figure 2.4 The procedure of microdiffusion preparation using conway cell (above) and typical chromatogram of free cyanide obtained by IC-PAD method (below).	9
Figure 2.5 Schematic illustration of the sensing mechanism for the detection of cyanide based on the fluorescent and colorimetric properties of AuNPs...	10
Figure 2.6 Schematic representation of cyanide detection.	11
Figure 2.7 Mechanism of the vitamin B ₁₂ based cyanide sensor.	12
Figure 2.8 Structure of corrinoids.	13
Figure 2.9 CTAB structure and CTAB aggregate forms.	14
Figure 2.10 Different morphologies that may form during the adsorption of soluble CTAB from low to high coverage (left to right) onto a clean hydrophilic substrate (silica).....	15
Figure 4.1 Different morphologies of CTAB that may form during the adsorption of high concentration CTAB to a clean hydrophilic substrate (silica).....	27
Figure 4.2 Thermogram of silica gel, CTAB and CTAB-coated silica	28
Figure 4.3 FT-IR spectra of an uncoated-silica gel (a) and CTAB-coated silica (b)	29
Figure 4.4 Absorption spectra of phenanthroline (blue line), Fe(II) (orange line), ferroin (gray line), and a mixture of ferroin and 100 μ M cyanide (yellow line).....	30

Figure 4.5 DR-UV absorption spectra of raw CTAB-coated silica and CTAB-coated silica used to extract cyanide of different concentrations.	31
Figure 4.6 Scheme of cyanide detection.	32
Figure 4.7 Calibration curve for cyanide determination using 0.167, 0.20 and 0.25 mM of ferroin reagent	34
Figure 4.8 Calibration curve for cyanide determination using 15, 20 and 25 mL of sample volume.....	36
Figure 4.9 Expected mechanism of cyanide detection in CTAB-containing media.....	39
Figure 4.10 Material color at 1 and 5 minutes of extraction time	41
Figure 4.11 Calibration curve for cyanide determination constructed from results obtained at 1 and 5 minutes of extraction time.	41
Figure 4.12 Calibration curve obtained from using different concentrations of ferroin.....	43
Figure 4.13 Calibration curve for cyanide determination using ferroin and CTAB-modified silica and material color chart.....	45
Figure 4.14 The color intensity observed in the detection of cyanide in standard solution in the absence (cyanide blank) and in the presence of various foreign ions (1 mM).....	47
Figure 4.15 External calibration curve and standard addition calibration curve for determination of cyanide in water sample.....	48
Figure 4.16 Color of materials used to detect cyanide in standard solution and in different spiked water samples.	49

LIST OF SCHEMES

	page
Scheme 3.1 The analytical procedure for cyanide colorimetric detection.....	20



LIST OF ABBREVIATIONS

M	Molar
mM	Millimolar
mg/L	Milligram per liter
µg/L	Microgram per liter
mL	Milliliter
°C	Degree Celsius
ppm	Part per million
ppb	Part per billion
LOD	Limit of detection
TGA	Thermal gravimetric analysis
CTAB	Cetyltrimethylammonium bromide
KCN	Potassium cyanide
NaCN	Sodium cyanide
NaNO ₃	Sodium nitrate

CHAPTER I

INTRODUCTION

1.1 Statement of background and problem

Cyanide is one of the most well-known toxic chemicals. It can be described as any chemical compound that contains the cyano group ($C\equiv N$). Cyanide compounds could be solid, liquid or gas and the most toxic species is free cyanide (CN^-) or HCN gas. They are rapid-acting poison and cause sudden-death. Inorganic cyanide salts such as NaCN, KCN are crystalline solid and also highly toxic. [1] On the other hand, metal cyanide complexes such as $Fe(CN)_6^{3-}$, $Cu(CN)_2^-$, $Co(CN)_2$, $Au(CN)_4^-$ are less toxic due to the strong interaction between metal atom and cyanide ion.[2] Cyanide originates from either natural or anthropogenic source. The major problem about cyanide contamination in the environment is human activities such as cigarette smoke, incomplete combustion of plastic or fire accident, electroplating process, tanning process, metallurgy, use of insecticides, and especially mining industrial of gold and silver. [3-6] The contamination would be in air, soil, and water. Cyanide toxicity on humans includes its effects on iodine uptake to thyroid gland, on nervous system and respiratory system etc.[7] According to the toxicity of cyanide, there are announcement of the maximum level of cyanide allowed in drinking water of 200 $\mu\text{g/L}$, 50 $\mu\text{g/L}$, and 50 $\mu\text{g/L}$ set by the US EPA, European Union, the World Health Organization, respectively.[7-9]

The monitoring cyanide level is necessary in particular in the area of contamination. The techniques for cyanide determination include ion chromatography, potentiometry and amperometry with cyanide-selective electrodes, and spectrophotometry.[10-12] However, these techniques require the transport of sample to the laboratory, expensive equipment, skillful technician, and hence the process is time-consuming. For on-site detection, it needs techniques that are simple, rapid, portable equipment. The colorimetric determination by using simple spectroscopic technique or naked-eyes is an interesting alternative[13] to provide preliminary results at the field.

The colorimetric detection of cyanide is generally based on complex formation as cyanide is a chelating ligand. The reactions such as metal cyanide complex formation would result in a change of color or optical properties.[14] Several complexation reactions including Prussian blue complex[15], complex with vitamin B₁₂ [16] and dicyano-bis-(1,10-phenanthroline)-iron(II) complex[17] were applied in the colorimetric detection and the results could be observed by naked eyes. Moreover, several methods as UV-Visible spectroscopy, fluorescent spectroscopy, Diffuse Reflectance Spectroscopy (DR-UV vis) are used for quantitative analysis.[18-21]

This research is focused on the colorimetric detection of cyanide on solid using tris(1,10-phenanthroline)-iron(II) (Ferroin) as a reagent. The obtained neutral complex of dicyano-bis-(1,10-phenanthroline)-iron(II) has purple color. This reaction was applied to detect cyanide at microgram level when the complex was extracted into organic solvent phase and analyzed by UV-Vis spectrophotometer. To avoid the use of toxic organic solvent, solid phase extraction and preconcentration concept are adopted in this work. CTAB-coated silica is chosen as solid material that exhibits non-polar surface for extracting the neutral dicyano-bis-(1,10-phenanthroline)-iron(II) complex. Furthermore, silica can be coated with cetrimonium bromide (CTAB) through the interaction between silanol groups and positive head of CTAB.[22] CTAB hydrophobic tail makes this material surface become more non-polar and suitable for the extraction of hydrophobic compound. The color of the material changes from pale orange to purple in the presence of cyanide and it can be observed by naked eyes. The color intensity is also determined by image-J program to obtain quantitative data. The method was applied to detect cyanide in water samples.

1.2 Research objective

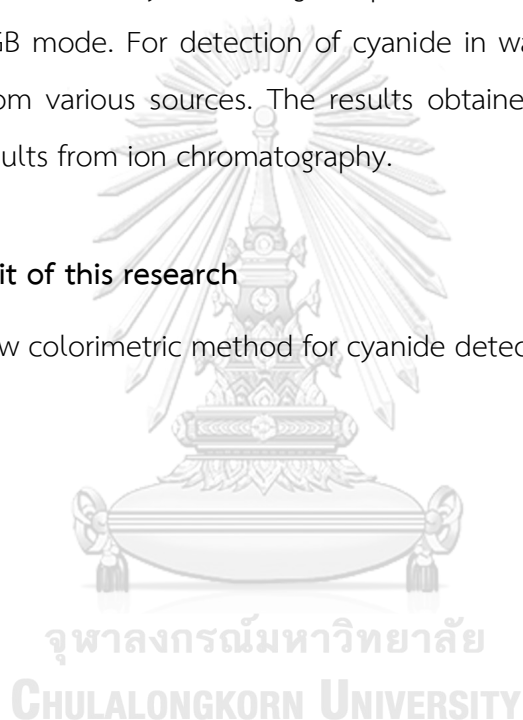
- 1.2.1 To develop a colorimetric method for determination of cyanide.
- 1.2.2 To apply the method to detect cyanide in water samples.

1.3 Scope of the research

For this method, the concentration of cyanide in the range of 30-150 μM was chosen. Various parameters which affect the cyanide detection were studied such as the concentration of ferriin, sample volume, CTAB concentration in complex formation step, extraction time, ferriin concentration used to form complex in CTAB media. Furthermore, the effect of foreign anions including fluoride, chloride, bromide, iodide, sulfate, carbonate, iodate, and thiocyanate was also studied. The color intensity of material was determined by submitting the photo to image J program to measure the intensity in RGB mode. For detection of cyanide in water samples, the samples were collected from various sources. The results obtained from this method were compared with results from ion chromatography.

1.4 The benefit of this research

To obtain a new colorimetric method for cyanide detection in water sample.



CHAPTER II

THEORY AND LITERATURE REVIEW

2.1 Cyanide

Cyanide can be described as chemical compound which contains the cyano group ($C\equiv N^-$). [23] Cyanide compound can be in different form such as solid, liquid or gas depending on their sources i.e. natural and anthropogenic source. [24] One of the most toxic cyanide compounds is hydrogen cyanide (HCN) (pK_a 9.22). HCN is a colorless or pale blue liquid or gas with bitter almond smell. It is rapidly adsorbed into human body through inhalation, ingestion, and skin contact. Breathing of cyanide gas in the level of 100-300 ppm would cause death within 10-60 minutes and death can come more quickly upon an increase of concentration. [25] Other compounds are cyanide salts such as sodium or potassium cyanide which are crystalline hygroscopic salts. Cyanide salts can be absorbed to digestive track by consuming of contaminated food. [26] Toxicity of cyanide to human depends on the type of chemical compound that releases cyanide anion. NaCN or KCN are highly toxic because the affinity of cyanide anion with alkaline metals is low and thus cyanide ion was released easily. On the other hand, the affinity between cyanide and heavy metal is high such as in $FeCN_2$, $CuCN$. Consequently, low amount of cyanide is released from these compounds, thus this form would be less toxic. Primary toxic effect of cyanide is that it affects to metalloenzyme by impairing enzyme and cell function. The activity of cytochrome c oxidase which contains iron atom is inhibited by cyanide ion and then electrons transport from cytochrome c to oxygen is prevented. As a result, the cell cannot aerobically produce ATP for energy and it eventually causes tissue damage. [27] Additionally, it also causes thyroid hormone decreasing by interfering iodine uptake to thyroid gland. [28] Low level of cyanide will cause headache and dizziness, while its high level will affect central nervous system and respiratory system and finally cause death. [29]

Cyanide can be released from natural or anthropogenic source. For anthropogenic source, cyanide is largely released from mining of valuable elements such as gold or silver via Elsner's reaction (eq. 2.1).[30]



For natural sources, cyanogenic glycoside could be found in many plants such as cassava, lima beans, almonds or bamboo shoots as shown in Fig 2.1. Hydrogen cyanide is released from enzymatic hydrolysis of cyanogenic glycoside when fresh plants are chewed and mixed with enzyme in mouth. However, the processing of these plants by soaking, boiling, cooking, fermentation, drying or roasting has been reported to reduce amount of cyanogenic glycoside.[31]

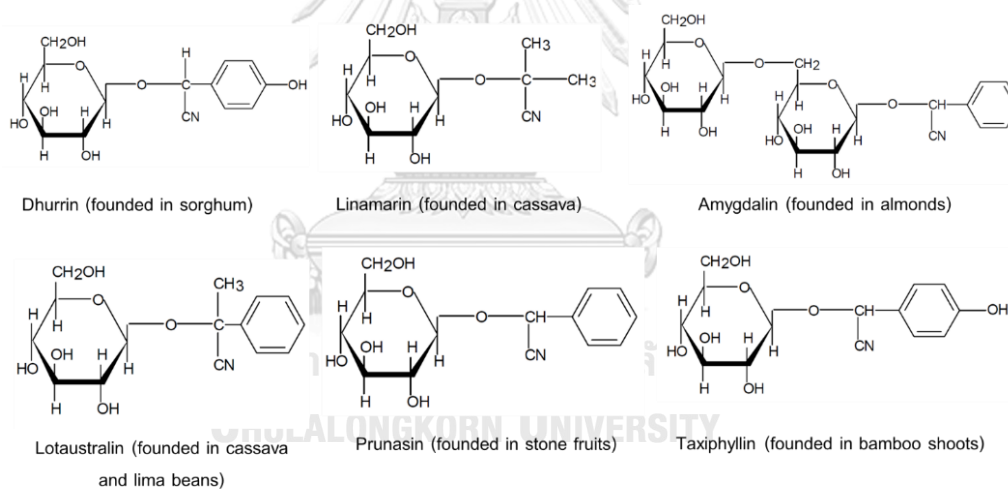


Figure 2.1 Cyanogenic glycosides in plants.[31]

For cyanide detoxification in living organism are shown in Fig 2.2. About 80% of uptake cyanide is metabolized in the liver and transformed to thiocyanate (SCN^-) which is less toxic and released with urine. Moreover, cyanide could form complex with vitamin B_{12} and cystine to obtain products in stable form. [32]

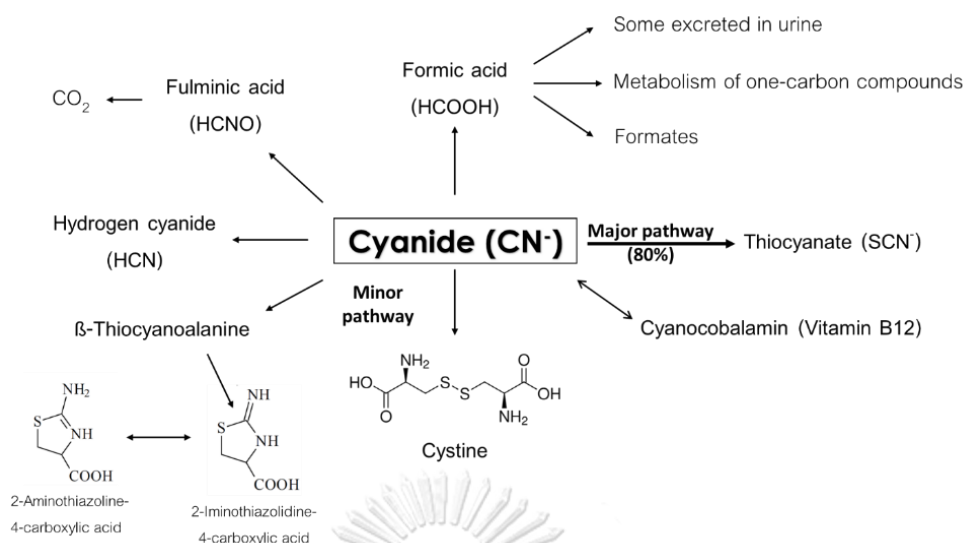


Figure 2.2 Process of cyanide metabolism in living organism.[24]

In nature, cyanide compounds tend to migrate easily through soils and may leach into groundwater. In 1974, Congress passed the Safe Drinking Water Act that requires US EPA to set the regulation about the maximum level of contaminants in drinking water.[33] The maximum level of cyanide contaminant in drinking water set by the US EPA, European Union, the World Health Organization is 200 µg/L, 50 µg/L, and 50 µg/L, respectively.[7-9]

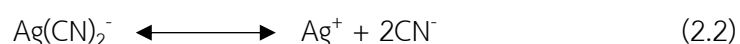
2.2 Methods for cyanide detection

For detection of cyanide in samples, many methods have been reported including electrochemical method, ion chromatography method, and colorimetric method which are explained hereafter in more details.

2.2.1 Electrochemical methods

The electrochemical methods for cyanide detection such as potentiometric method have been developed. This technique provides fast and sensitive detection. However, it is affected by many interferences such as halides, pseudohalides, sulfide, and metal cyanide complexes and response of electrode may change over time.[34]

Kameswara and co-workers [11] presented a method for detecting hydrogen cyanide gas by using a pair of silver electrodes which one was kept in silver dicyano complex at pH 11.5 and another one was the reference electrode. The silver electrodes responded to silver ions concentration present in the solution due to the equilibrium shown in eq. 2.2.



The detection was based on the potential difference between the two electrodes when hydrogen cyanide gas passed into the cell. The linear calibration was in the concentration range from 0.66–42.3 mg/m³ and LOD was 0.66 mg/m³. The potential interferences were hydrogen sulfide and hydroiodic acid as they formed silver sulfide and silver iodide precipitates layer on the silver metal wire and changed its function from a silver electrode to that of Ag/Ag₂S and Ag/AgI electrode.

Vallejo-Pecharromán and Luque[35] developed an automated system for the determination of total cyanide in water samples. HCN was generated by photodissociation of Fe(CN)₆³⁻. Then HCN was pervaporated and collected in dilute NaOH solution for the measurement by ion-selective electrode. The detection limit for total cyanide was 0.01 µg/L.

Amayreh and Abulkibash[36] applied differential electrolytic potentiometry (DEP) using silver electrodes coated with carbon nanotubes as a detector for cyanide determination by flow injection analysis system. The direct current differential electrolytic potentiometry (dc-DEP) and the mark-space bias differential electrolytic potentiometry (m.s.b. DEP) were performed. For dc-DEP, a linear range of 1 to 65 ppm of cyanide, LOD of 0.5 ppm, and a relative standard deviation of 2.1% were obtained. On the other hand, in m.s.b. DEP method, a linear range of 1 to 65 ppm of cyanide, LOD of 0.35 ppm, and a relative standard deviation of 1.5% were observed.

2.2.2 Ion chromatography

An ion chromatography with pulsed amperometric detection (IC-PAD) is one of the most popular method due to its high sensitivity and selectivity. This method is based on the separation of components in the sample by the ion affinity toward the ion exchanger and using electrical conductivity as a detector.[37] However, this method is time consuming and it requires high skill technician and expensive equipment. Examples of cyanide detection by ion chromatography are listed below.

For cyanide detection in water sample, Christison and Rohrer[10] described direct determination of free cyanide in drinking water by ion chromatography method with pulsed amperometric detection (PAD). Samples was treated with NaOH and transition metals ions was removed by a cation-exchange cartridge before the analysis. The recovery was higher than 80% with method detection limit of 1 $\mu\text{g/L}$.

Destanoglu and co-workers[38] developed pretreatment and chromatographic methods for the analysis of cyanide trace in drinking water and seawater. Separation of CN^- in the form of CNO^- and other anions was performed by using Dionex IonPac AS20 column. LOD and LOQ values were 7.2 ppb and 24.0 ppb for drinking water and 15.4 ppb and 51.3 ppb for sea water, respectively. The spiked recovery of 250 ppb cyanide in drinking water was found to be 100.1% and 100.1 % at 50 ppb spike level in sea water. Moreover, the interferences were removed by using strong acid cation-exchange resin and melamine-formaldehyde resin. The obtained chromatogram is shown in Fig 2.3.

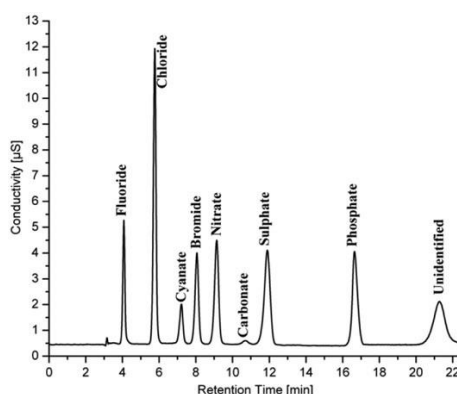


Figure 2.3 Chromatogram of cyanate (1 ppm) and other anions.

For cyanide detection in plant samples, in 2018, Ding and Wang[39] developed a practical method for the determination of cyanide in bamboo shoots by using microdiffusion preparation integrated with ion chromatography–pulsed amperometric detection (IC-PAD) (Fig. 2.4). The linear range for cyanide determination was 0.2–200.0 $\mu\text{g}/\text{kg}$ and the LOD was 0.2 $\mu\text{g}/\text{kg}$ ($S/N=3$). The spiked recovery ranged from 92.8 to 98.6%. Relative standard deviations of results obtained intra-day and inter-day were 2.7–14.9% and 3.0–18.3%, respectively.

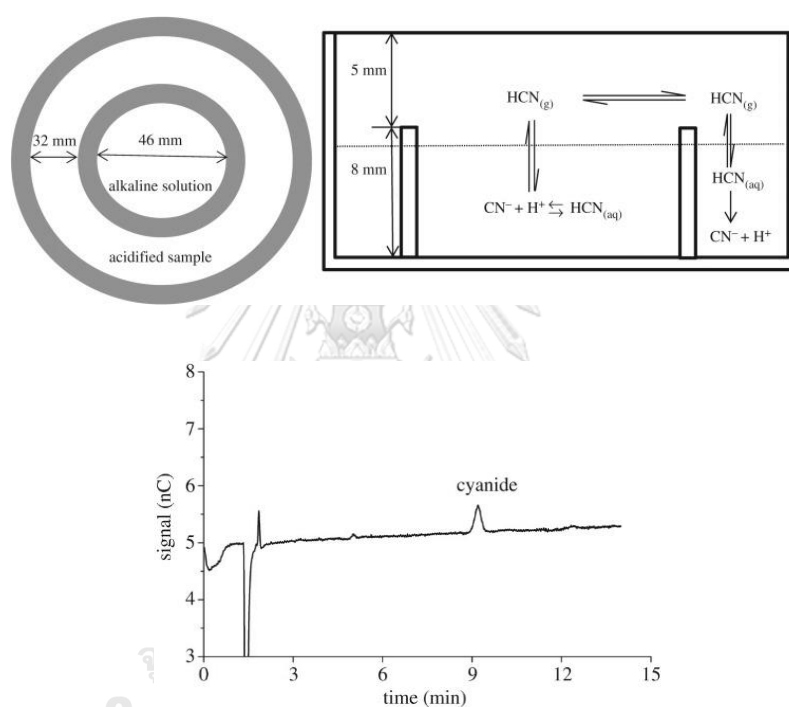


Figure 2.4 The procedure of microdiffusion preparation using Conway cell (above) and typical chromatogram of free cyanide obtained by IC-PAD method (below).

2.3 Colorimetry and spectrophotometry

The colorimetric detection of cyanide has become more popular due to simple and easy procedure and inexpensive equipment. In addition, the detection can be performed on-site. Generally, the method is based on the change of optical properties of complexes or aggregation of metal nanoparticles in solution, on material or on paper. The colorimetric method can be used for qualitative, semi-quantitative, and quantitative analysis of cyanide by several techniques including UV-Visible spectroscopy, fluorescence spectroscopy, and naked-eye detection.[34]

Cheng and co-workers [14] proposed an application of fluorescent and colorimetric cyanide sensor using gold nanoparticles (AuNPs) modified with fluorescein isothiocyanate (FITC; fluorescent dye). The modified AuNPs solution did not give fluorescence. In the presence of cyanide at low concentration, cyanide would form soluble gold-cyanide complex and etching of AuNPs occurred. Consequently, FITC was released from the surface of AuNPs and enhanced the fluorescence intensity of solution. However, at high concentration of cyanide, AuNPs was aggregated and displayed a blue-gray color of AuNPs in solution (Fig. 2.5). For the fluorescence method, LOQ was 1.0×10^{-7} M. When cyanide concentration was higher than $150 \mu\text{M}$, UV-Visible method was applied in working range of $150\text{-}300 \mu\text{M}$ of cyanide.

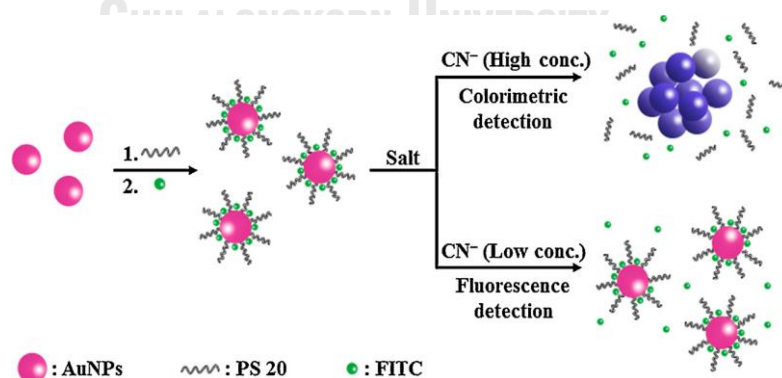


Figure 2.5 Schematic illustration of the sensing mechanism for the detection of cyanide based on the fluorescent and colorimetric properties of AuNPs.

Kaushik R. and co-workers[12] used off-the-shelf chemical 6,7-dihydroxycoumarin based copper complex ($1 \cdot \text{Cu}^{2+}$) to detect cyanide in water and biological samples. The mechanism of this method is based on the fluorescence turn on in the presence of cyanide ions. The complex of 6,7-dihydroxycoumarin and Cu^{2+} did not give fluorescence (fluorescence “off”). When cyanide ions were present, it can coordinate with Cu^{2+} ions in ($1 \cdot \text{Cu}^{2+}$) and release 6,7-dihydroxy coumarin which has fluorescent properties (fluorescence “on”) as shown in Fig 2.6. The binding of cyanide towards Cu^{2+} in $1 \cdot \text{Cu}^{2+}$ complex was confirmed by UV-Vis absorption and fluorescence emission spectra. LOD of cyanide detection was $5.77 \mu\text{M}$ and $14.4 \mu\text{M}$ in water and fresh mouse serum, respectively. Furthermore, this method was applied to detect cyanide in cell by treating the cell with $1 \cdot \text{Cu}^{2+}$ and fluorescence cell imaging was observed.

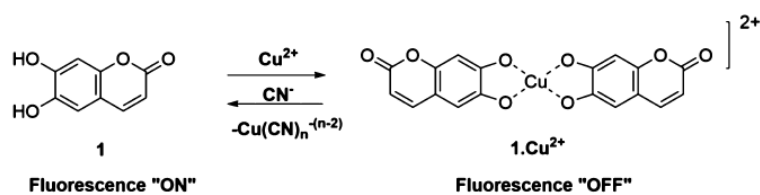


Figure 2.6 Schematic representation of cyanide detection.

Bhowmick and co-workers[40] developed naked eye detection of cyanide in water with Co^{II} bis(terpyridine) complexes. The new Co^{III} tricyanide complex [Co^{III} (4-pyridyl-terpyridine)(CN)₃] occurred. The results showed color change from orange to mostly colorless. The quantitative detection of cyanide was monitored by UV-Vis spectroscopic. The Co^{II} -bis-terpyrine based complex was found to be highly selective and sensitive for naked eye colorimetric detection of $10 \mu\text{M}$ cyanide in water.

Felix H. Zelder[18] developed a colorimetric detection of cyanide in water using vitamin B₁₂. This method is based on the binding of cyanide ion with vitamin B₁₂ and its optical properties change was detected by UV-Visible spectroscopy and naked-eye (Fig 2.7). The color of vitamin B₁₂ changed from red to violet in the presence of

cyanide ion. Moreover, this method was highly sensitive (LOD 600 μM) and highly selective toward cyanide detection over other anions.

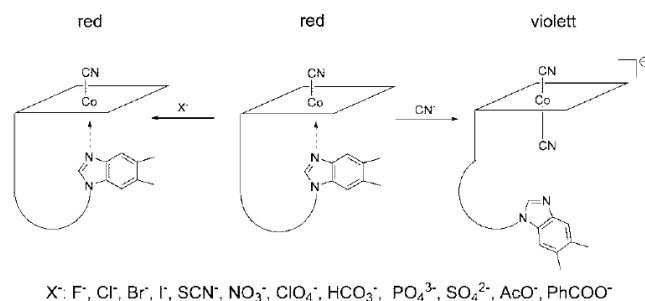


Figure 2.7 Mechanism of the vitamin B₁₂ based cyanide sensor.

Vitamin B₁₂ has been further applied for cyanide detection in different type of samples. Chaudhary and co-workers[16] used vitamin B₁₂ for colorimetric detection of cyanide in blood by loading vitamin B₁₂ onto filter paper for detecting HCN released from acidified blood sample. The color of filter paper changed from red to purple due to the presence of dicyanocobalamin which was the product of vitamin B₁₂ and cyanide. The limit of detection of this method was 1.0 mg/L and the method was highly selective toward hydrogen cyanide over other common gas such as NH₃, CO₂, CO, AsH₃, and PH₃.

The cyanide detection on paper-based platform has been developed in order to fit the application on-site. Gholamzadeh and co-workers[13] synthesized and used 1,4-Bis(2,2-dicyanovinyl) benzene as cyanide chemosensor. The color in solution changed from light yellow to purple in the presence of cyanide and its color intensity depended on cyanide concentration. The solution was measured by UV-Visible spectroscopy and the limit of detection was 3.07×10^{-7} M. Furthermore, the chemosensor was applied onto filter paper. To detect cyanide in solution, the chemosensor-loaded paper was dipped in sample solutions. The result showed that among various anions, only cyanide changed color from light yellow to purple. This method is highly sensitive and selective.

Furthermore, colorimetric detection of cyanide on solid has been developed. Colorimetric detection on solid is based on complex formation or aggregation of

nanoparticle on solid surface or extraction the complex onto solid material. It can be used as test kit for on-site detection.

Mannel-Croise and Zelder[21] designed colorimetric solid phase with spatially separated extraction and detection zones for the optical detection of cyanide in samples with complex matrix. It is used for detection of endogenous cyanide in colored plant samples and hydrogen cyanide in tobacco smoke. The principle of this work is to immobilize corrinoids on C18-silica gel due to the good adsorption properties for corrinoids. Cyanide would substitute Co(III) coordinated water (eq. 2.3) and cause a color change from orange to violet with a characteristic maximum absorption at 583 nm in the reflection spectrum.



For practical use, they tested cyanide in raw extracts of cassava leaves. The extraction zone containing C18-silica gel was built to separate green color from leaves and connected to the detection zone which contains corrinoids-immobilized C18-silica gel as shown in Fig 2.8. The green color remained on separation zone and endogenous cyanide was found in the detection zone. Moreover, it was also applied for detection of hydrogen cyanide in tobacco smoke. For quantitative determination, the solid in the detection zone was separated and analyzed by diffuse reflectance spectroscopy (DR-UV-vis) and linear range was up to 0.2 mg/L with a LOD of 1 µg/L.

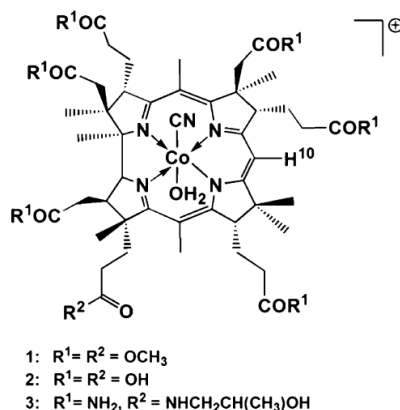


Figure 2.8 Structure of corrinoids.

From the literature review, the colorimetric determination of cyanide is widely performed either in aqueous media or on paper-based platform, while a few of solid colorimetric detection of cyanide is reported. In this study we were interested in using solid sorbent as material for naked eye detection of cyanide ion in water samples. Silica was chosen as material due to its high surface area and good physical properties. The silica was modified with cetyltrimethylammonium bromide (CTAB) to produce hydrophobic surface for cyanide complex extraction and detection.

2.4 Modification of silica with CTAB

Cetyltrimethylammonium bromide (CTAB) is a cationic surfactant. It is a white powder with a melting point of 237 - 243 °C and critical micelle concentration (CMC) of 1 mM.[41] CTAB has bulky positive hydrophilic head and hydrophobic tail. Self-assembly of CTAB will occur in solution at concentration higher than its CMC. The aggregation of CTAB will be in various morphologies such as spherical micelles, wormlike micelles, vesicles, and lipid bilayers as shown in Fig 2.9.[42] CTAB was used in various studies as stabilizer of gold nanoparticle[43], as template for synthesizing mesoporous silica[44], and used to coat on solid surface in order to enhance the dispersion of the particles in solution[45]. Different solids such as magnetic nanoparticles (Fe_3O_4), silica gel, aluminar, clay, ilmenite or silica/polyamide-imide nanocomposite thin films was applied and coated with CTAB.[45-49] Moreover, CTAB-PVP was also used to modify silica to extract high quality genomic DNA from a single larva or pupa.[50]

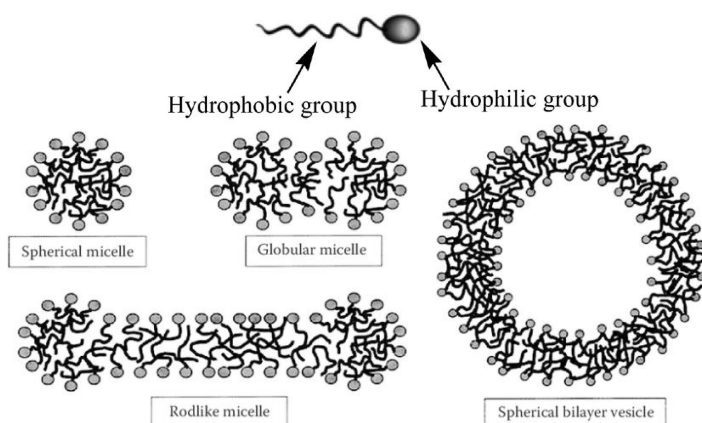


Figure 2.9 CTAB structure and CTAB aggregate forms.[51]

The adsorption of cationic surfactant onto hydrophilic substrate has been studied. There are various morphologies that may form during the adsorption of surfactant onto a clean hydrophilic substrate (1d) as shown in Fig 2.10. At very low coverage, the surfactant monomers may randomly lie on the substrate (1a-1c). As the concentration increases, the molecules may form a single layer (Langmuir behavior, 2c) or interactions between surfactant molecules occur and hemimicelles (2a) or admicelles (2b) was formed. At high coverages, the surfactant may form a monolayer (3a) when concentration is lower than its CMC or hemimicelles on a monolayer (3b), bilayer (3c), admicelles (3d) when concentration is higher than its CMC.

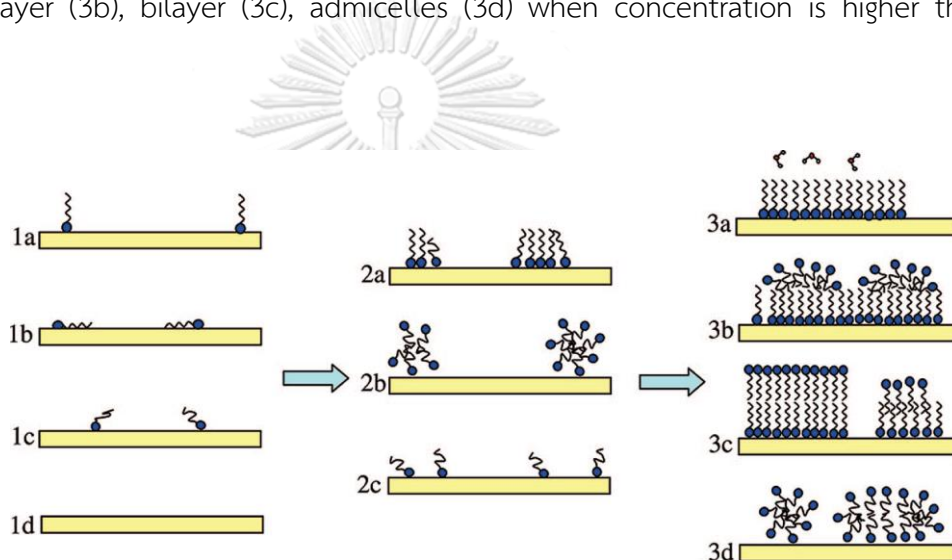


Figure 2.10 Different morphologies that may form during the adsorption of soluble CTAB from low to high coverage (left to right) onto a clean hydrophilic substrate (silica) [22]

2.5 Quantitative analysis using value color space

Colors are the characteristic of visual perception that could be determined by spectroscopic techniques or color spaces. Color spaces defined color from three primary colors which are similar to human perception. The RGB color space represents color used by devices e.g. scanner, digital camera. All the colors are represented as a combination of red, green and blue primaries. Spectrum of three regions are used to calculate the intensity of each color channels. The spectral responsivity of the blue, green, and red channels are roughly Gaussian functions with typical ranges of 400-500, 500-580, and 580-700 nm, respectively. The value for a channel indicates the total photons in that region as given by eq. 2.4, 2.5 and 2.6; [52]

$$R = \int_{\lambda} P(\lambda)S_R(\lambda) d\lambda \quad (2.4)$$

$$G = \int_{\lambda} P(\lambda)S_G(\lambda) d\lambda \quad (2.5)$$

$$B = \int_{\lambda} P(\lambda)S_B(\lambda) d\lambda \quad (2.6)$$

where,

P is incident intensity

S is spectral responsivity for a particular channel

CHAPTER III
EXPERIMENTAL

3.1 Chemicals

All of the chemicals were of analytical reagent (AR) grade. The list of chemicals is shown in table 3.1. Milli Q water was used as solvent to prepare all solutions in this study.

Table 3.1 List of chemicals

Chemicals	Supplier
Silica gel 60 (70-230 mesh)	Merck, Germany
Hexadecyltrimethylammonium bromide (CTAB)	Fluka analytical, United States
Potassium cyanide	Merck, Germany
Potassium dihydrogen phosphate	Merck, Germany
1,10-Phenanthroline	Sigma-Aldrich, United States
Ferrous ammonium sulfate	Allied Chemical, United States
Hydroxylammonium chloride	Merck, Germany
Sodium hydroxide	Merck, Germany
Sodium nitrate	CARLO ERBA, Italy
Sodium fluoride	CARLO ERBA, Italy
Sodium chloride	Fisher Scientific, United States
Potassium bromide	Merck, Germany
Sodium iodide	CARLO ERBA, Italy
Sodium sulfate	Merck, Germany
Sodium bicarbonate	Merck, Germany
Potassium iodate	Sigma-Aldrich, United States
Potassium thiocyanate	CARLO ERBA, Italy

3.2 Instruments

Table 3.2 List of instruments

Instrument	Model
Fourier-transform infrared spectroscopy (FT-IR)	Nicolet 6700 FT-IR Spectrometer, Thermo Scientific, United States
Diffuse reflectance ultraviolet visible spectrophotometer (DR-UV)	UV-2500 Shimadzu, Japan
Ion chromatography	Thermo Scientific Dionex Integriion RFIIC system, United States
Pipette	Brand transferpette, Germany
Camera	Sony a5100
Zeta potential	Zeta sizer V 7.04
Thermal gravimetric analyzer (TGA)	PerkinElmer Pyris 1 TGA, United States
Magnetic stirrer	Gem/MS 101, Germany
Centrifuge	Universal 320 HETTICH, Germany
pH meter	Orion2Star, Thermoelectron, Taiwan
UV-Visible spectrophotometry	Hewlett Packard model HP 8453, Germany

3.3 Preparation and characterization of CTAB-coated silica

3.3.1 Preparation of CTAB-coated silica

Silica gel (1.00 g) was mixed with 100 mM CTAB solution (100 mL) and the pH of the mixture was adjusted to 10 by using 1.0 M of NaOH solution. The mixture was stirred for 1 hour and the solution was discarded. The CTAB-coated silica was washed by Milli Q water once and dried at 80 °C for 12 hours.

3.3.2 Characterization of CTAB-coated silica

To confirm that CTAB could be extracted onto the silica gel, the modified silica was characterized by IR, TGA and zeta potential, compared to bare silica.

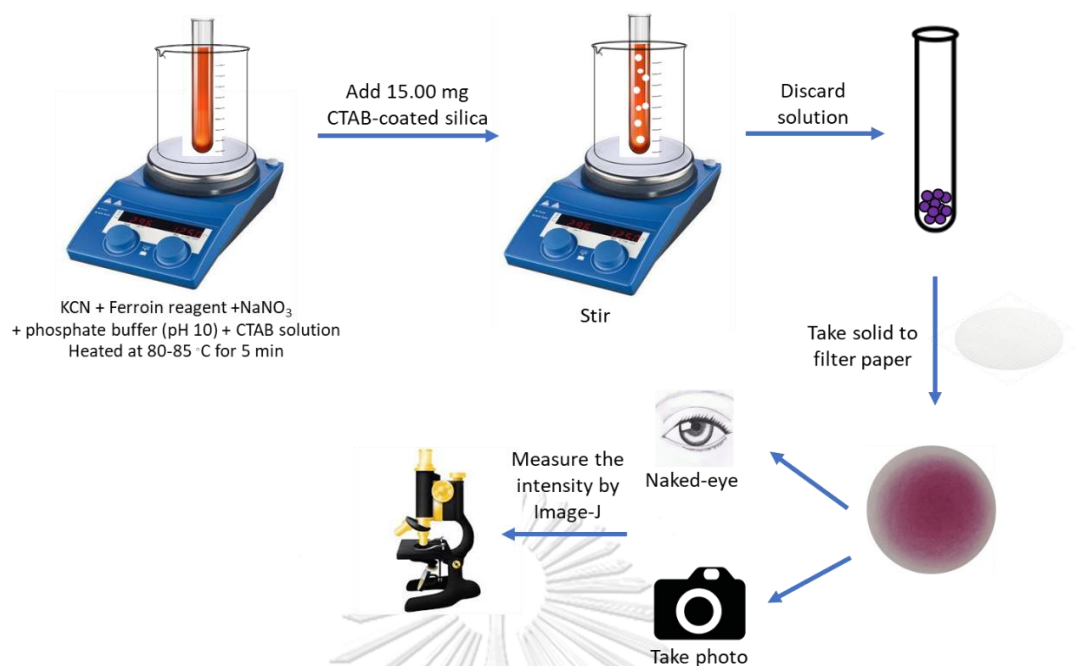
3.4 Preparation of ferroin reagent

To prepare 0.025 mM ferroin stock solution, 245.10 mg of $\text{FeSO}_4(\text{NH}_4)_2\text{SO}_4 \cdot 6\text{H}_2\text{O}$ was dissolved in 10 mL of Milli Q water. Then, 1 mL of 10%wt hydroxylamine solution was added, followed by 337.89 mg of phenanthroline. The volume of the mixture was adjusted to 25.00 mL with Milli Q water. The obtained ferroin reagent solution was characterized by a UV-Visible spectrophotometer, compared to $\text{FeSO}_4(\text{NH}_4)_2\text{SO}_4$ and phenanthroline solution.

3.5 Colorimetric determination of cyanide

3.5.1 Cyanide detection

Stock solution of KCN was prepared in Milli Q water. Standard KCN solution was mixed with phosphate buffer and NaNO_3 to get the mixture that contained cyanide of desired concentration, 0.05 mM phosphate buffer (pH 10), and 0.05 mM NaNO_3 solution. Ferroin of specific concentration was added and then heated at 80-85 °C for 5 minutes. After heating, CTAB-coated silica (15.00 mg) which was previously conditioned with a small amount of ethanol was added into the mixture and stirred. The solid was separated for color observation. The photo of the solid was taken in a lighting studio box and imported to Image-J program for measuring the color intensity. In addition, the materials were characterized by a diffuse reflectance ultraviolet visible spectrophotometer (DR-UV-vis) in a wavelength range of 400 to 800 nm to confirm the extraction of complex onto the material. The method of cyanide determination is schematically shown in Scheme 3.1.



Scheme 3.1 The analytical procedure for cyanide colorimetric detection

3.5.2 Optimization of cyanide determination method

To obtain the optimal condition for cyanide detection, the effect of several parameters including ferriin concentration, CTAB concentration (complex formation step), extraction time and ferriin concentration used to form complex in CTAB media were investigated. The range of values of the studied parameters is presented in Table 3.3.

จุฬาลงกรณ์มหาวิทยาลัย
CHULALONGKORN UNIVERSITY

Table 3.3 The range of values of studied parameters for cyanide detection

Parameters	Range of values
Ferriin concentration used to form complex	0.167 - 0.25 mM
Sample volume	15 – 25 mL
CTAB concentration (complex formation step)	0.1 – 10 mM
Extraction time	1 – 10 minutes
Ferriin concentration used to form complex in CTAB media	0.15 – 0.25 mM

3.6 Method performance

The performance characteristic of the method such as accuracy, precision, limit of detection, linear working range was determined. The effect of foreign ions was also evaluated under optimal condition.

3.6.1 Linear working range

The external calibration curve for cyanide detection was constructed from results obtained under optimal condition. The calibration curve was plotted between mean of green intensity of the material color as y-axis against cyanide concentration in the range of 30-150 μM as x-axis. Furthermore, the linear regression was used with the data and the correlation coefficient value (R^2) was determined.

3.6.2 Limit of detection

The limit of detection (LOD) of the method was obtained by the measurement of blank solution which contained phosphate buffer (pH 10) and 0.05 mM of NaNO_3 as medium. The experiment was performed followed section 3.5.1 under the optimum condition in ten replicates. The color intensity of the obtained material was measured by using ImageJ program and recorded in green scale. In our case, in the absence of cyanide, the color of the material was pale yellow or orange and the green values were high. On the other hand, when the material turned pink in the presence of cyanide, low green values were observed. The color intensity obtained at LOD concentration was calculated by the mean value acquired from blank solution analysis (I_{blk}) minus three times of standard deviation (SD_{blk}) ($n=10$) according to Eq.3.1;

$$I_{\text{LOD}} = I_{\text{blk}} - 3SD_{\text{blk}} \quad (3.1)$$

where,

I_{LOD} = the color intensity of silica used in solution at LOD concentration

I_{blk} = the mean of color intensities of silica used in blank solution

SD_{blk} = the standard deviation of color intensities of silica used in blank solution

The level of LOD was obtained by comparing I_{LOD} values to the standard calibration curve plotted between color intensity (mean green values) and concentration of cyanide in range of 30 – 150 μM .

3.7 Effect of foreign ions

The effect of foreign in the cyanide detection in water sample with the purposed method was studied. Foreign anions including fluoride, chloride, bromide, iodide, sulfate, carbonate, iodate, and thiocyanate were mixed with cyanide standard solutions (50 and 100 μM) to prepare binary mixture. The level of these anions was 1 mM. These mixtures were analyzed by the proposed method and the results were compared to that observed in cyanide standard solutions.

3.8 Determination of cyanide in water samples

In the analysis of cyanide in real sample, water samples were collected from several sources and analyzed by the method describes in section 3.5.1 under the optimum condition.

3.8.1 Effect of water sample matrix

To evaluate the effect of water sample matrix on cyanide detection, the external calibration curve and the standard addition calibration curve were compared. The external calibration curve was built by using the analytical results from the analysis of cyanide standard solution, while standard addition calibration curve was constructed from the data obtained from spiked water sample with final spike concentration of 30, 50, 80, 100, and 150 μM cyanide. The green intensity of material color was measured by ImageJ and used for constructing calibration curves.

3.8.2 Accuracy and precision in water sample analysis

Owing to the effect of sample matrixes, the standard addition method was adopted to overcome the effect. Cyanide standard solutions of different concentrations were added into a set of 15.00 mL of water samples with a fixed volume to create a set of spiked samples. To evaluate the accuracy of the method, the spiked water sample was analyzed under optimal condition and the recovery of cyanide was determined. Cyanide standard solution was added into water samples to reach the spike concentration of 30 μM and 50 μM in samples. Percent recovery can be calculated using Equation 3.2. Percent recovery of the spiked analyte should be in the range 80-110 % for the acceptable accuracy of method as shown in Table 3.4 according to the AOAC International criteria [53],

$$\% \text{ recovery} = \frac{X_s - X_b}{S} \times 100 \quad (3.2)$$

where,

- X_s is the concentration of cyanide found in the spiked sample
- X_b is the concentration of cyanide found in non-spiked sample
- S is the spike concentration of cyanide in the sample

The precision of this method was presented in term of percentage of relative standard deviation (%RSD) value which should not be higher than 11 % (Table 3.4) based on the AOAC International criteria.

Table 3.4 Percent recovery and percent RSD of analytical results obtained at different analyte concentrations according to AOAC international

Analyte (%)	Mass fraction	Unit	Recovery range (%)	RSD (%)
100	1	100%	98-102	1.3
10	10 ⁻¹	10%	98-102	1.9
1	10 ⁻²	1%	97-103	2.7
0.1	10 ⁻³	0.1%	95-105	3.7
0.01	10 ⁻⁴	100 ppm	90-107	5.3
0.001	10 ⁻⁵	10 ppm	80-110	7.3
0.0001	10 ⁻⁶	1 ppm	80-110	11
0.00001	10 ⁻⁷	100 ppb	80-110	15
0.000001	10 ⁻⁸	10 ppb	60-115	21
0.0000001	10 ⁻⁹	1 ppb	40-120	30

In addition, the acquired analytical results from the proposed method were compared to the results from ion chromatography. The same samples were analyzed by an ion chromatograph with the analytical conditions shown in Table 3.5. The external calibration method was applied to determine cyanide by ion chromatography. Furthermore, the detail of camera and the condition of taking pictures are listed in Table 3.6.

Table 3.5 List of conditions of ion chromatography method

Parameters	Values
Column	Dionex IonPac AG 19 (4 x 50 mm) guard column and Dionex IonPac AS 19 (4 x 250 mm) separation column, that packed with alkanol quaternary ammonium
Eluent	KOH (10 mM)
Flow rate	1.0 mL/min
Injection volume	25 μ L
Detector	Conductivity detector

Table 3.6 Details of camera condition

Conditions	Details
Camera maker	SONY
Camera model	ILCE-6000
F-stop	f/5.6
Exposure time	1/640 sec.
ISO speed	ISO-100
Focal length	50 mm
Max aperture	4.96875
Metering mode	Center Weighted Average
Flash mode	No flash, compulsory
35mm focal length	75

CHAPTER IV

RESULTS AND DISCUSSIONS

In this research, a colorimetric method is proposed for the determination of cyanide in water samples. The method is based on the reaction of cyanide ions and tris(1,10-phenanthroline)-iron(II) (ferroin) at pH 10. This condition is the most suitable for complex formation and to keep cyanide in its anionic form (pK_a HCN = 9.31). [17, 54] The reaction occurs through ligand exchange reaction[55] to give a neutral complex of dicyano-bis-(1,10-phenanthroline)-iron(II) ($\text{Fe}(\text{phen})_2(\text{CN})_2$) which has purple color as shown in eq 4.1.



To increase the sensitivity of the detection, CTAB-coated silica is used to extract and preconcentrate the $\text{Fe}(\text{phen})_2(\text{CN})_2$ complex. Silica gel was coated with CTAB using 100 mM CTAB solution at pH 10.[47] Under this condition, silica surface would be deprotonated and hence the adsorption of CTAB occurs through electrostatic interaction of this cationic surfactant with anionic active site on silica. The efficiency in CTAB adsorption would increase, compared with the coating at neutral pH. The adsorption time was 1 hour to assure that the adsorption equilibrium is attained. After coating the silica with CTAB, the silica surface would exhibit hydrophobic properties due to non-polar part of CTAB covered on the surface. As a result, the complex could be extracted onto the silica and the material color turned to purple. However, the ferroin reagent could also be adsorbed on CTAB-coated silica and produce the orange color on the solid. Therefore, the color on material changed from orange in the absence of cyanide to purple in the presence of cyanide.

4.1 Material characterization

In this work, the obtained materials, reagent, and complex were characterized by several techniques as described in detail as follows.

4.1.1 Characterization of CTAB-coated silica

In this work, the silica was coated with 100 mM CTAB solution. This condition was adapted from the work of Xiaokun Ma and co-workers which they modified silica nanoparticles by CTAB to improve the dispersal state of the silica nanoparticles in the polyamide-imide matrix.[47] More importantly, this concentration is higher than the critical micelle concentration of CTAB (CMC 1 mM) and CTAB would form micelles in solution.[56] CTAB could be adsorbed onto silica surface through interaction between their cationic head group and silanol group with different possibility of morphologies including hemimicelles on a monolayer, bilayer or admicelles as shown in Fig 4.1.[22] Furthermore, this concentration of CTAB which is the highest solubility of CTAB[57] in aqueous solution is chosen to assure the maximum coverage of CTAB on silica surface.

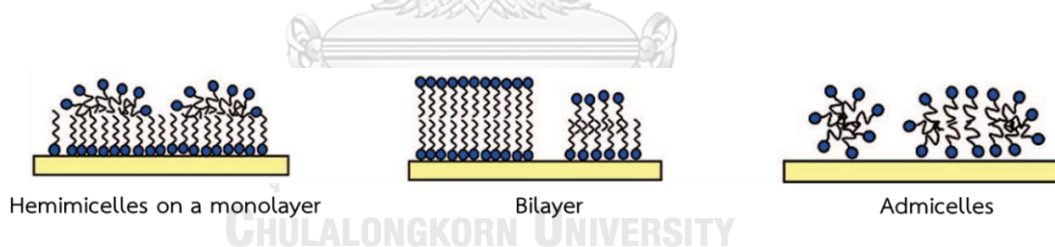


Figure 4.1 Different morphologies of CTAB that may form during the adsorption of high concentration CTAB to a clean hydrophilic substrate (silica) [22]

To confirm the presence of CTAB on silica surface, the thermal stability of silica gel, CTAB and CTAB-coated silica were investigated by TGA and compared. The weight-loss was observed in the temperature range of 50-400 °C at a heating rate of 10 °C/min under nitrogen atmosphere and the thermograms are shown in Fig 4.2. The decomposition of CTAB was observed at temperature starting from 259.18 °C to 280 °C which is higher than its melting point (m.p. 237 - 243 °C).[57] The thermogram of CTAB-coated silica showed a weight loss at temperature above 215.82 °C, while

raw silica did not show any weight loss. The weight loss observed in CTAB-silica thermogram could be attributed to the decomposition of organic moiety on silica which was probably CTAB due to similar decomposition temperature range.

The results indicated that the CTAB-coated silica was successfully prepared. Percent weight loss of CTAB-coated silica was 26.3% and the content of CTAB was calculated to be 262.95 mg/g silica.

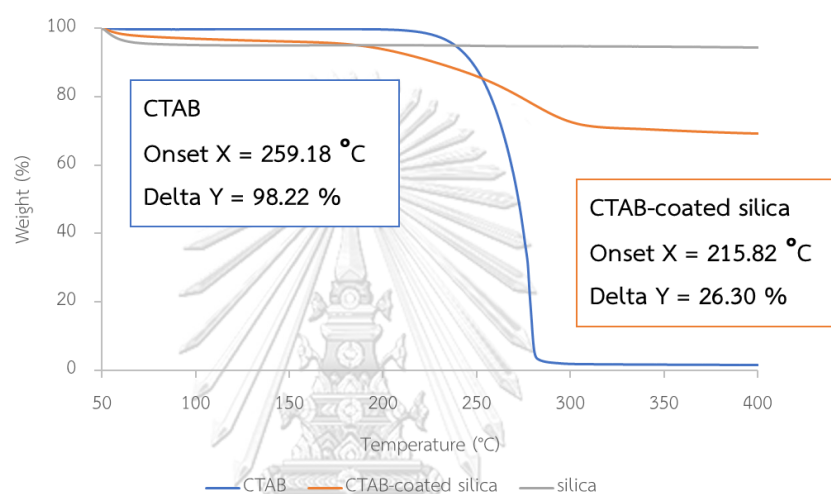


Figure 4.2 Thermogram of silica gel, CTAB and CTAB-coated silica

To examine functional groups on the materials, silica and CTAB-coated silica was analyzed by FT-IR and the obtained spectra are shown in Fig 4.3. The characteristic vibrations of Si-O at 1,050, 960 and 790 cm^{-1} were present in both spectra. On the other hand, the typical stretching vibrations of C-H at 2,917 and 2,850 cm^{-1} attributed to the $-\text{CH}_2$ and $-\text{CH}_3$ in CTAB molecule, were observed only in the spectra of CTAB-coated silica. It indicates that CTAB could be coated onto silica surface.

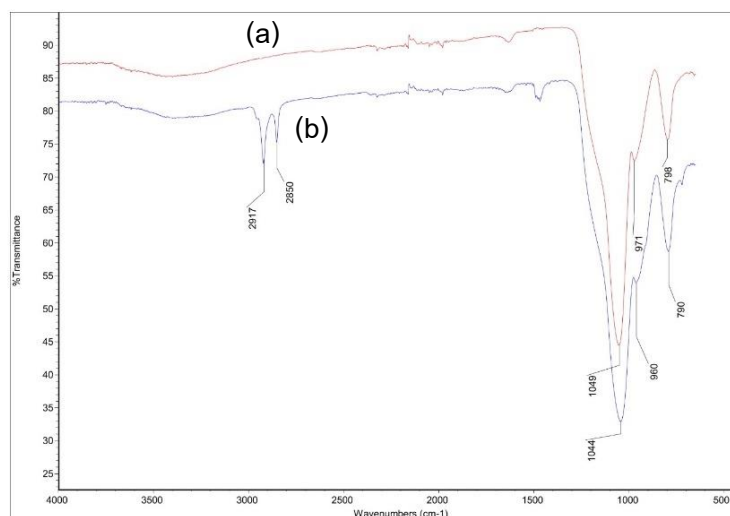


Figure 4.3 FT-IR spectra of an uncoated-silica gel (a) and CTAB-coated silica (b)

4.1.2 Characterization of complexes

In an attempt to confirm the formation of ferriin and dicyano-bis-(1,10-phenanthroline)-iron(II) complex in solution, a solution of phenanthroline, Fe(II), Ferriin, and a mixture of ferriin and 100 μ M cyanide solution were analyzed by UV-Vis spectrophotometer and the obtained UV-Visible absorption spectra are shown in Fig 4.4. The absorption band of phenanthroline was found at 200-325 nm, while a new absorption band at 430-550 nm was observed in ferriin spectra with a maximum absorption at 510 nm. The results was in agreement with a previously reported spectra of ferriin.[58] In addition, the mixture of ferriin and cyanide solution showed similar absorption range with a red-shift of the absorption maxima. This could be dicyano-bis-(1,10-phenanthroline)-iron(II) which was reported to have absorption band in a region of 537-600 nm (λ_{\max} 597 nm).[17]

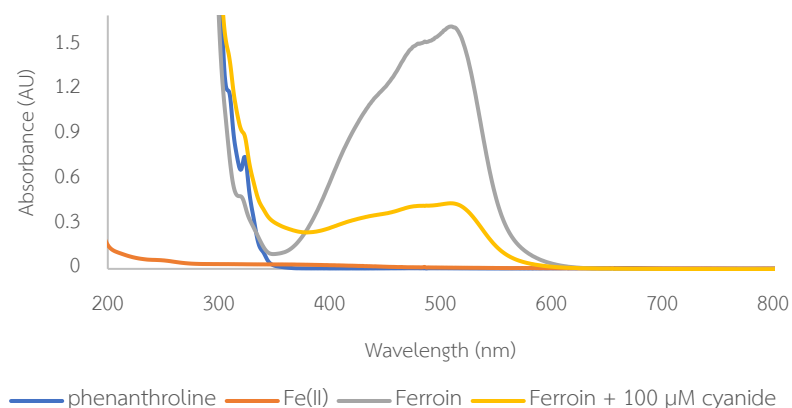


Figure 4.4 Absorption spectra of phenanthroline (blue line), Fe(II) (orange line), ferrioxin (gray line), and a mixture of ferrioxin and 100 μ M cyanide (yellow line).

Furthermore, the materials were characterized by a diffuse reflectance ultraviolet visible spectrophotometer (DR-UV-Vis) to check the presence of substance on the materials. The presence of $\text{Fe}(\text{phen})_2(\text{CN})_2$ complex on CTAB-coated silica used to extract the complex in solutions containing different concentrations of cyanide ions was observed as shown in Fig 4.5. The spectra of raw CTAB-coated silica did not show significant absorption. However, when it is used in a solution without cyanide, the absorption in the wavelength range of 500 to 600 nm was observed which would be attributed to the presence of ferrioxin extracted onto the material. In the presence of 50 and 150 μ M of cyanide, the absorption spectra of the used materials showed absorption band from 500 to 600 nm. These results show similar absorption region when compared with UV-visible spectra of complex in solution. Furthermore, the absorbance values increased corresponding to an increase of cyanide concentration. The results indicated that the extraction of a natural complex $\text{Fe}(\text{phen})_2(\text{CN})_2$ onto CTAB-coated silica was achieved probably by the interaction between the complex and the hydrophobic part of CTAB on silica surface.

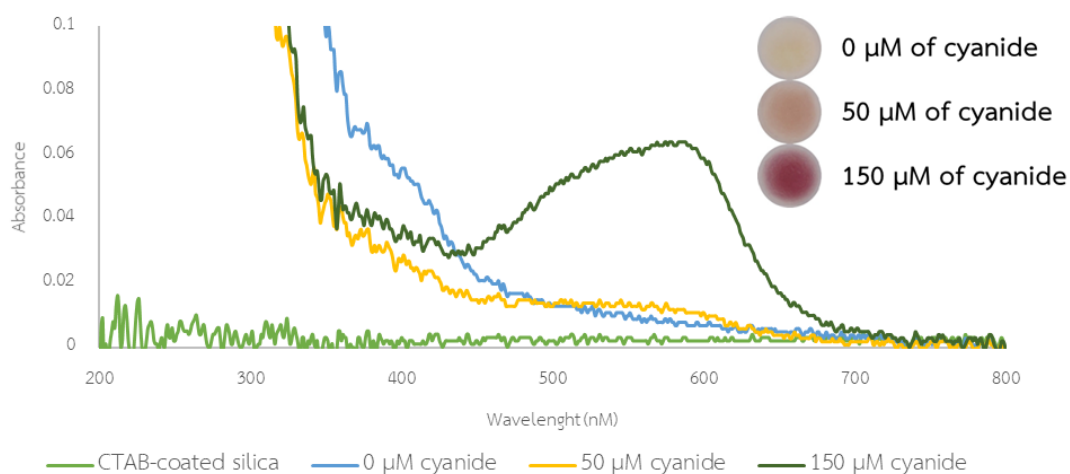


Figure 4.5 DR-UV absorption spectra of raw CTAB-coated silica and CTAB-coated silica used to extract cyanide of different concentrations.

4.2 Colorimetric detection of cyanide

In the detection of cyanide by this method, it started from the formation of $\text{Fe(phen)}_2(\text{CN})_2$ complex in solution (eq. 4.1) by adding ferriin reagent into cyanide solution. The solution color turned from colorless to orange because of the ferriin reagent color. Then, the mixture was heated to 80-85 °C for 5 minutes to accelerate the ligand exchange reaction. From the preliminary study, the complex formation reaction did not occur when performed at the room temperature despite the use of 24 hours reaction time. It was checked by extraction with chloroform and there was no purple color of complex in organic phase. Moreover, from the work of Alfred A. Schilt,[17] they stated that the formation of $\text{Fe(phen)}_2(\text{CN})_2$ complex was completed after heating around 5 minutes. However, a lower recovery of complex was observed when heated longer than 40 minutes at 100 °C. After heating, the solution still had orange color but paler than the starting color. Nevertheless, the purple color of $\text{Fe(phen)}_2(\text{CN})_2$ complex could not be observed by naked eyes probably due to low concentration of complex. Immediately after heating, the CTAB-coated silica was mixed with the mixture solution to extract the $\text{Fe(phen)}_2(\text{CN})_2$ complex and

purple color was observed on silica surface. The scheme of cyanide detection is shown in Fig 4.6.

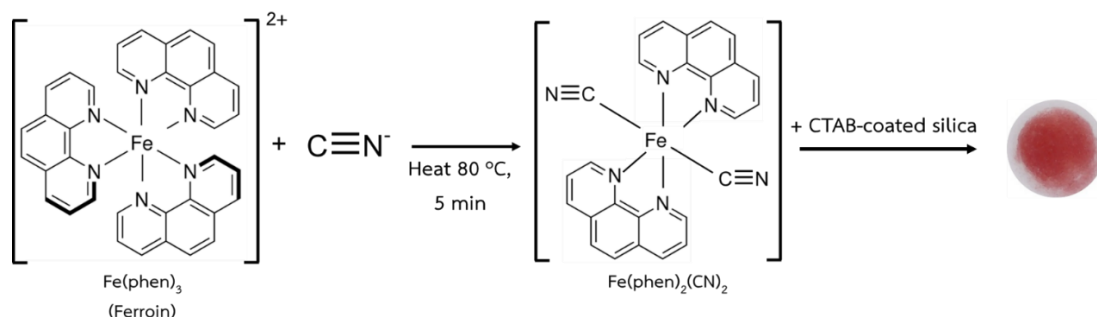




















Figure 4.6 Scheme of cyanide detection.

4.2.1 Effect of ferriin concentration

The effect of ferriin concentration on the detection of cyanide was investigated by varying the ferriin concentration from 0.167 to 0.25 mM with phosphate buffer at pH 10 and NaNO_3 as a medium. After extraction of $\text{Fe}(\text{phen})_2(\text{CN})_2$ complex onto CTAB-coated silica for 1 minute, the solid color was observed as shown in Table 4.1. The material color changed from orange to red-purple upon an increase of cyanide concentration. The suitable concentration of ferriin was selected based on the color change on the material and the obtained calibration curve plotted between color intensity and cyanide concentration. By naked eyes detection, red-purple color was obviously observed starting from 80 μM of cyanide by using 0.167 mM ferriin, and from 50 μM of cyanide by using 0.20 and 0.25 mM ferriin, respectively. However, when 0.25 mM ferriin was applied, the material color was intense orange due to a high amount of free ferriin on surface. Consequently, it is difficult to distinguish the material color by naked eyes. These ferriin residue was likely absorbed on silica via the interaction with silanol groups which were not covered by CTAB.

Table 4.1 Effect of ferroin concentration on the color of the material used in the detection of cyanide in a concentration range of 0-120 μM

Ferroin conc. (mM)	CN^- concentration (μM)					
	0	30	50	80	100	120
0.167						
0.20						
0.25						

(condition: 15 mg of CTAB-coated silica, 20 mL of sample volume, 1 minute of extraction time)

The color intensity of the solid was measured by submitted the photo of the solid to Image J program. The RGB values were recorded for each solid photo and used for calibration curve construction. The calibration curve of results obtained from using different ferroin concentrations were plotted by using green intensity of the material color against cyanide concentration and compared. The results are shown in Fig 4.7. According to the linear regression of results, the obtained calibration curves showed that the sensitivity in cyanide detection increased upon an increase of ferroin concentration and a similar sensitivity was obtained by using 0.20 and 0.25 mM of ferroin. Considering the color change observed by naked eyes and the sensitivity in cyanide detection under this experimental condition, a 0.20 mM ferroin solution was chosen as reagent for further study.

According to the results, upon an increase of ferroin concentration, lower concentration of cyanide could be detected and higher sensitivity was obtained. It indicated that the complex formation of $\text{Fe}(\text{phen})_2(\text{CN})_2$ would be more favorable by increasing of ferroin concentration due to increasing of ferroin and cyanide mole ratio. For example, under this experimental condition, at 50 μM of cyanide, ferroin and

cyanide mole ratio increased from 3.3 to 4.0 and 5.0 when the concentration ferrioin was raised from 0.167 mM to 0.20 mM and 0.25 mM, respectively.

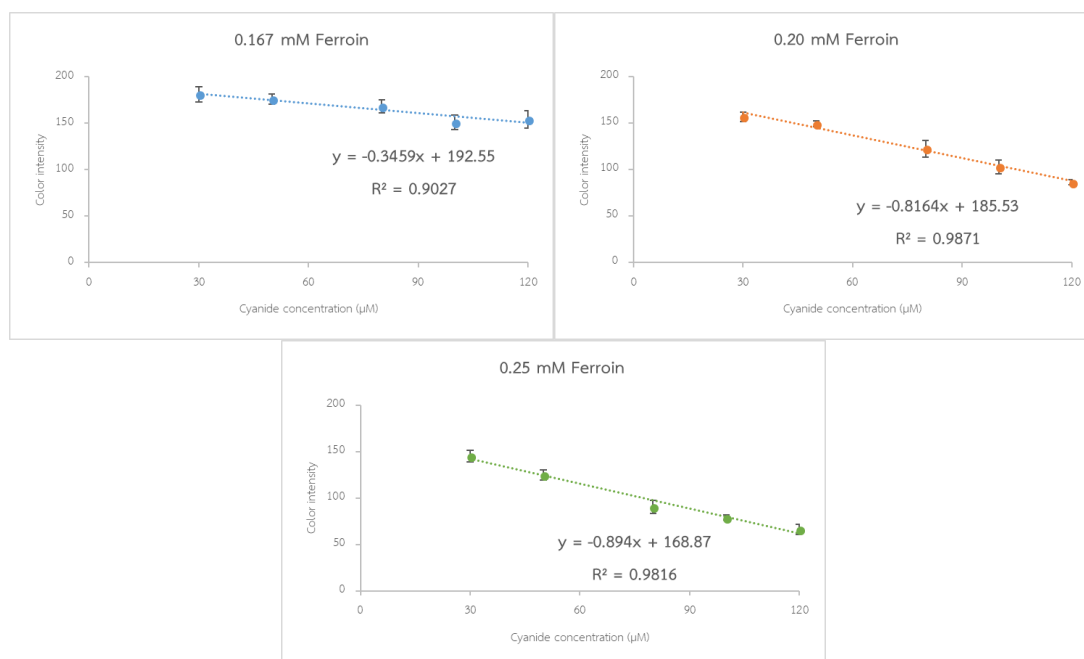








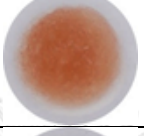





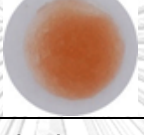

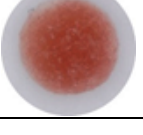



Figure 4.7 Calibration curve for cyanide determination using 0.167, 0.20 and 0.25 mM of ferrioin reagent

4.2.2 Effect of sample volume

To obtain a high sensitivity of detection, the effect of sample volume was investigated. The sample volume was varied in the range from 15.00 to 25.00 mL for the detection of cyanide by using 15 mg of CTAB-coated silica. The color of materials after the complex extraction from sample of different volumes is shown in Table 4.2. The results show that increasing of sample volume in the studied range slightly affected the change of complex color on material. When using 15 and 20 mL sample volume, the color of materials obtained from the analysis of cyanide of different concentrations were similar. Surprisingly, the color was slightly faded upon an increase sample volume to 25.00 mL, compared to the others. The calibration curves were constructed by using green intensity of the material color against cyanide concentration and compared as shown in Fig 4.8.

Table 4.2 Effect of sample volume on the color of the material used in the detection of cyanide in a concentration range of 0-120 μM

Sample volume (mL)	CN^- concentration (μM)					
	0	30	50	80	100	120
15						
20						
25						

(condition: 15 mg of CTAB-coated silica, 1 minute of extraction time, 0.20 mM ferriin)

According to linear regression of results, using a sample volume of 15 and 20 mL resulted in similar sensitivity regarding the slope of linear calibration curve. On the other hand, the results obtained in increasing sample volume to 25 mL showed lower sensitivity than those of other volumes. When sample volume was increased, the solid-liquid ratio in the extraction process changed. In this study, the ratio changed from 1:1.08 to 1:1.43 and 1:1.80, when sample volume changed from 15 mL to 20 and 25 mL, respectively. It is likely that the adsorption behavior of the complex onto the silica altered when the ratio changed under the fixed adsorption time. Since using 15 and 20 mL of sample volume with 15 mg CTAB-coated silica gave similar results, a sample volume of 15.00 mL was chosen for further study.

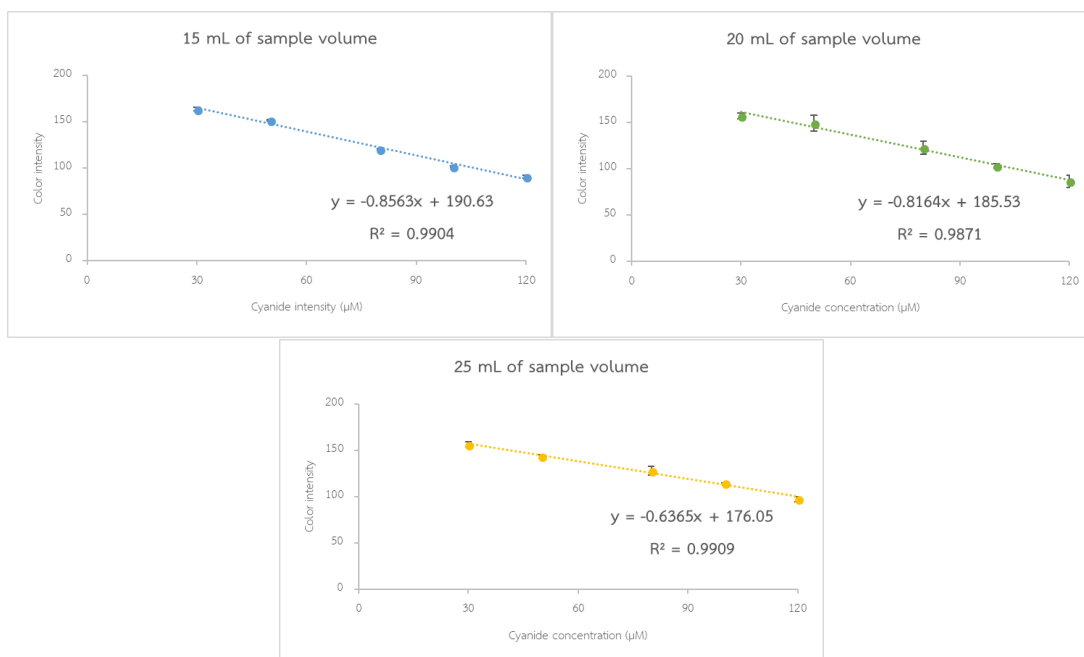





























Figure 4.8 Calibration curve for cyanide determination using 15, 20 and 25 mL of sample volume

4.2.3 Effect of CTAB concentration used in complex formation step

According to the previous results, the intense background color due to high amount of ferroin residuals on the material was the major problem encountered. This problem is a possible cause of low sensitivity in cyanide detection and it was difficult to distinguish the color change at low level of cyanide. To overcome this problem, CTAB solution was added into sample solution during complex formation step. The hypothesis is that CTAB in solution would entrap $\text{Fe}(\text{phen})_2(\text{CN})_2$ resulting in a better extraction of complex onto CTAB-coated silica surface. Moreover, as CTAB has positive head groups, it could be adsorbed onto silica surface through interaction with free silanol groups. Consequently, there was competitive adsorption of CTAB and ferroin onto silica and would result in less adsorption of ferroin.

In this experiment, CTAB was added to sample solution during complex formation step to get the final concentration of CTAB at 0.1 to 10 mM. Table 4.3 shows the color of silica gel and CTAB-coated silica after the extraction of the complex from mixture containing different concentrations of CTAB with 1 minute of extraction time.

Table 4.3 Effect of CTAB concentration added during complex formation step on the color of silica gel and CTAB-coated silica used in the detection of cyanide

CTAB conc. (mM)	Silica gel			CTAB-coated silica		
	CN ⁻ concentration (μM)			CN ⁻ concentration (μM)		
	0	50	100	0	50	100
0						
0.1						
1						
5						
10						

(condition: 15 mg of CTAB-coated silica, 15 mL of sample volume, 1 minute of extraction time, 0.20 mM ferroin)

At the same concentration of CTAB in the mixture, silica gel had more intense orange color than CTAB-coated silica indicating that ferroin residue were adsorbed on the silica surface in higher extent than on CTAB-coated silica. It was difficult to observe the color of the cyanide complex on the silica gel surface due to intense ferroin color on it. Therefore, coating the silica surface with CTAB improved the adsorption selectivity towards $\text{Fe}(\text{phen})_2(\text{CN})_2$ complex and prevented some parts of surface from ferroin adsorption. For CTAB-coated silica, without CTAB or in the presence of 0.1 and 1.0 mM CTAB in sample mixture, the ferroin residue was still extracted onto the material. On the other hand, when CTAB concentration was increased to

5 and 10 mM, which was higher than its critical micelle concentration (1 mM), the orange color was pale and the purple color of $\text{Fe}(\text{phen})_2(\text{CN})_2$ could be clearly observed. These results could be explained by the entrapment of $\text{Fe}(\text{phen})_2(\text{CN})_2$ complex in CTAB micelle that could be extracted onto CTAB-coated silica more efficiently. The expected mechanism is shown in Fig 4.9.

According to the results obtained by using 5 mM and 10 mM of CTAB the sample mixture, the color of materials had purple tone which could be clearly observed better than the other conditions. The green intensities of material color obtained at $50\mu\text{M}$ of cyanide were 142.6 and 151.2 and at $100\mu\text{M}$ were 125.1 and 137.2 using 5 and 10 mM CTAB, respectively. The paler the purple color, the higher the green intensity would be. It indicated that using 10 mM CTAB resulted in a decrease of amount of $\text{Fe}(\text{phen})_2(\text{CN})_2$ complex on solid. It is likely because the complex would prefer to be dissolved in solution than adsorbed onto material at high concentration of CTAB in solution. Therefore, 5 mM CTAB is the most suitable concentration and it was chosen for further study.

The expected mechanism of cyanide detection in CTAB-containing media is shown in Fig 4.9. When CTAB was added into sample solution, $\text{Fe}(\text{phen})_2(\text{CN})_2$ complex would be dissolved inside CTAB micelle which is hydrophobic. In extraction step, when the sample mixture was mixed with CTAB-coated silica, $\text{Fe}(\text{phen})_2(\text{CN})_2$ complex in micelle was adsorbed onto material surface and purple color would be observed. $\text{Fe}(\text{phen})_2(\text{CN})_2$ complex in micelle was possibly adsorbed better on CTAB-coated surface than without micelle.

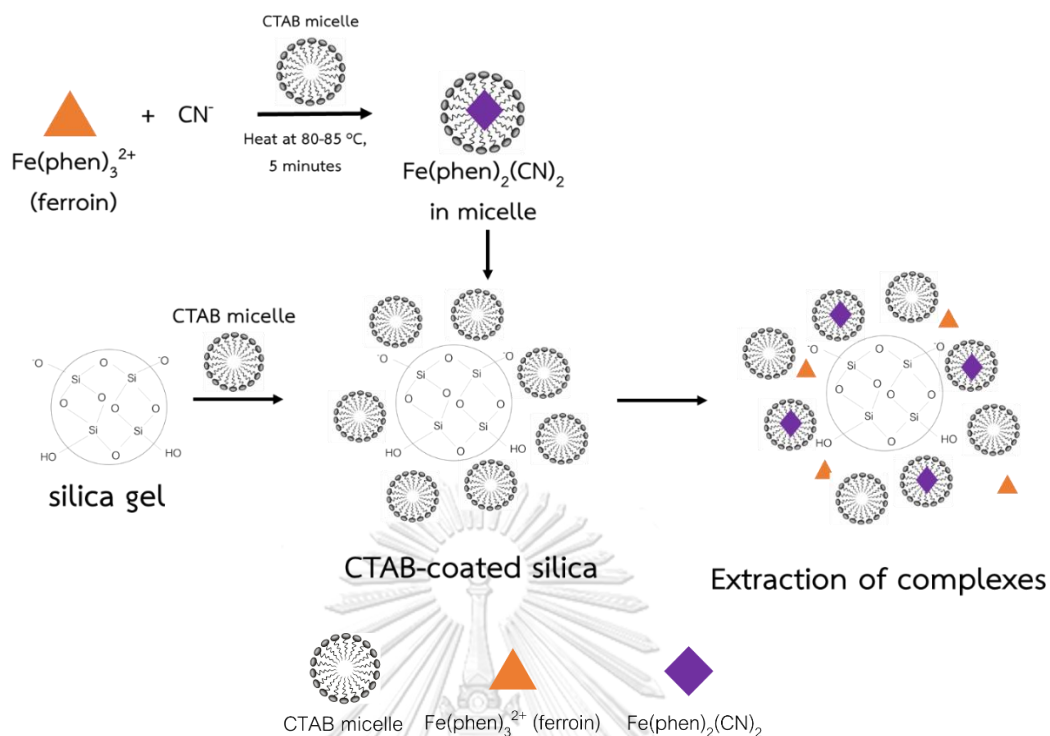














Figure 4.9 Expected mechanism of cyanide detection in CTAB-containing media

4.2.4 Extraction time

To obtain a suitable time to extract the complex from solution onto the material, the extraction time was varied from 1 to 10 minutes in the detection of cyanide. Table 4.4 shows that when the extraction time was 1 or 3 minutes, the orange color was still present on the material. But for 5 and 10 minutes, the orange color was much less pale and the purple color was more prominent. Under this condition, ferroin residual had concentration much higher than that of $\text{Fe(phen)}_2(\text{CN})_2$ complex and therefore, at the beginning, ferroin residual would be quickly extracted onto material. When the time length was longer, ferroin could be desorbed and replaced by $\text{Fe(phen)}_2(\text{CN})_2$ complex which had higher affinity towards CTAB-silica surface. Consequently, the amount of ferroin decreased while the content of $\text{Fe(phen)}_2(\text{CN})_2$ complex increased when prolonged the extraction time.

At 5 and 10 minutes, the material used to detect the same cyanide concentration had similar color when observed by naked eyes. These results had been confirmed by statistical calculation using t-Test and it showed that color intensities of the material used detect same cyanide concentration were not significantly different ($P= 0.538$ (50 μM cyanide) and $P= 0.933$ (100 μM)) at the 95% confidence level ($\alpha= 0.05$). The extraction time of 5 minutes was chosen for further study.

Table 4.4 Effect of extraction time used on the color of material used in the detection of cyanide in a concentration 0, 50 and 100 μM

Extraction time (minutes)	CN ⁻ concentration (μM)		
	0	50	100
1			
	141.7 \pm 7.5	140.6 \pm 4.9	123.0 \pm 5.2
3			
	162.2 \pm 0.7	136.7 \pm 2.9	95.8 \pm 6.8
5			
	172.8 \pm 0.8	151.5 \pm 2.9	110.9 \pm 3.6
10			
	172.8 \pm 0.9	153.1 \pm 3.1	111.2 \pm 4.2

(condition: 15 mg of CTAB-coated silica, 15 mL of sample volume, 0.20 mM ferrioin, 5 mM CTAB added in sample mixture)

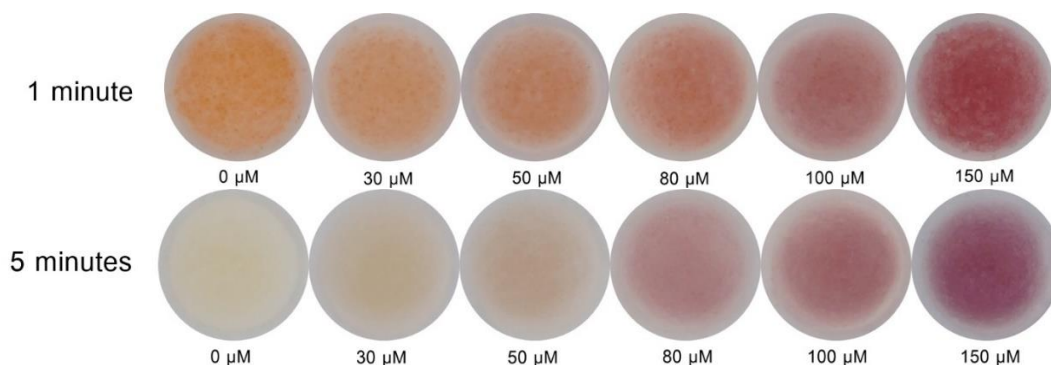


Figure 4.10 Material color at 1 and 5 minutes of extraction time

Figure 4.10 shows the color of material used in the detection of cyanide in a concentration range of 0 to 150 μM with different extraction time. At 1 minute of extraction time, the material showed more intense orange color compared to those observed at 5 minutes. To investigate the effect of extraction time on the sensitivity of detection, the calibration curve constructed from the results obtained from using 1 and 5 minutes of extraction time are compared in Fig 4.11. It was found that the linear relationship was obtained using the results from 5 minute of extraction time. On the other hand, the results from 1 minutes of extraction did not show a good linear relationship ($R^2 = 0.94$). It indicated that ferriin appearance on the material strongly affected the determination of cyanide.

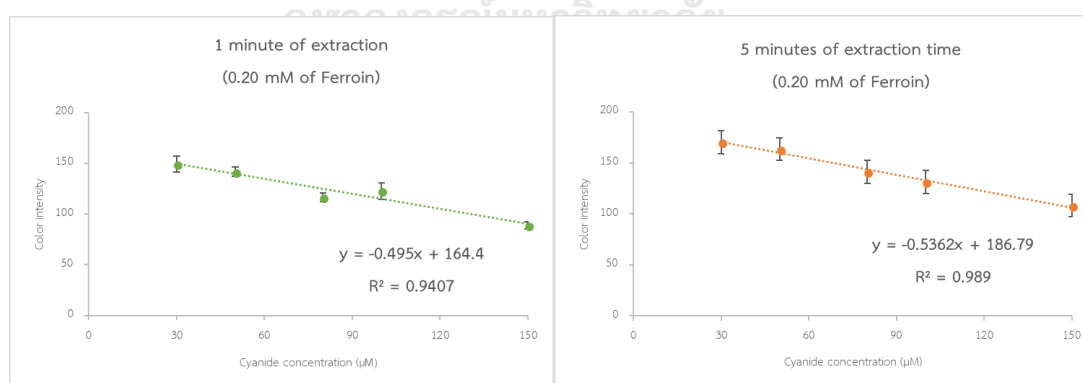


Figure 4.11 Calibration curve for cyanide determination constructed from results obtained at 1 and 5 minutes of extraction time.

4.2.5 Effect of ferroin concentration used in complex formation in CTAB-containing media

From the previous parameter, the problem of ferroin appearance had been solved. However, the color of complex at low concentration of cyanide was very pale. In an attempt to improve method sensitivity, the effect of ferroin concentration was reinvestigated by varying the ferroin concentration from 0.15 to 0.25 mM in the mixture of CTAB solution, phosphate buffer at pH 10, and NaNO_3 . The results are shown in Table 4.5. The suitable concentration of ferroin was selected based on the color change on the material and the color intensity related to the cyanide concentration. With every concentration of ferroin used, the material color changed from pale orange to purple corresponding to an increase of cyanide concentration. As expected, the silica showed more intense pink color of $\text{Fe}(\text{phen})_2(\text{CN})_2$ complex upon an increase of ferroin concentration. In addition, the calibration curves were constructed by using green intensity of the material color against cyanide concentration and compared in Fig 4.12. The results show that using 0.25 mM ferroin for cyanide detection gave a linear relationship between color intensity and cyanide concentration with the best sensitivity. Therefore, this concentration of ferroin was selected in this procedure.

Table 4.5 Effect of ferriin concentration used in complex formation in CTAB-containing media on the color of material used in the cyanide detection in a concentration range of 0-150 μM

Ferriin conc. (mM)	CN^- concentration (μM)					
	0	30	50	80	100	150
0.15						
0.20						
0.25						

(condition: 15 mg of CTAB-coated silica, 15 mL of sample volume, 5 mM CTAB added to sample mixture, 5 minutes of extraction time)

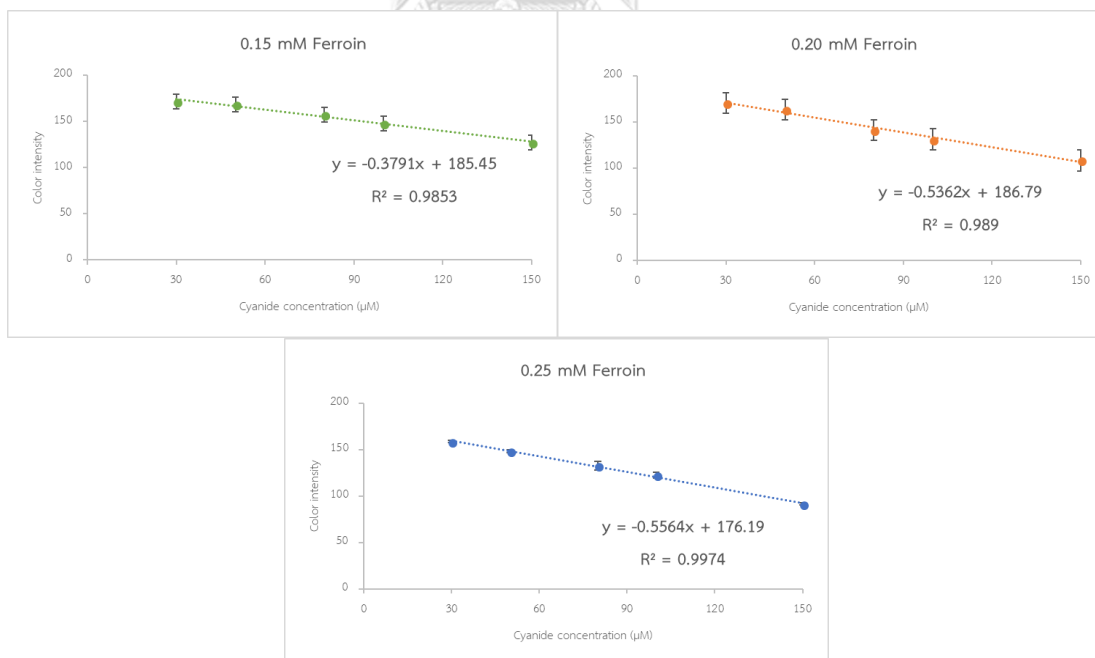


Figure 4.12 Calibration curve obtained from using different concentrations of ferriin

4.3 Method performance

In this section, the performance of the proposed method was evaluated under the chosen condition as followed. The cyanide ions in standard solution or sample (15 mL) formed $\text{Fe}(\text{phen})_2(\text{CN})_2$ complex in the media containing 0.25 mM ferroin, 5 mM of CTAB, and 0.05 M NaNO_3 . After heating the mixture at 80-85 °C for 5 minutes, 15 mg of CTAB-coated silica was added to extract $\text{Fe}(\text{phen})_2(\text{CN})_2$ complex for 5 minutes. The solid was separated and the color of material was observed by naked eyes. The color intensity of the solid was measured by submitted the photo of the solid to Image J program. The RGB values were recorded and used for calibration curve construction. Under this condition, the linear working range and the limit of detection (LOD) were determined.

4.3.1 linear working range

The linear relationship between color intensity in gray, red, green or blue scale and cyanide concentration was achieved in the concentration range of 30-150 μM as shown in Fig 4.13. According to the linear calibration curve, the results in green scale gave the most sensitive method for detection. The material color observed at each concentration of cyanide is also presented. This method was applied to detect cyanide in water samples.

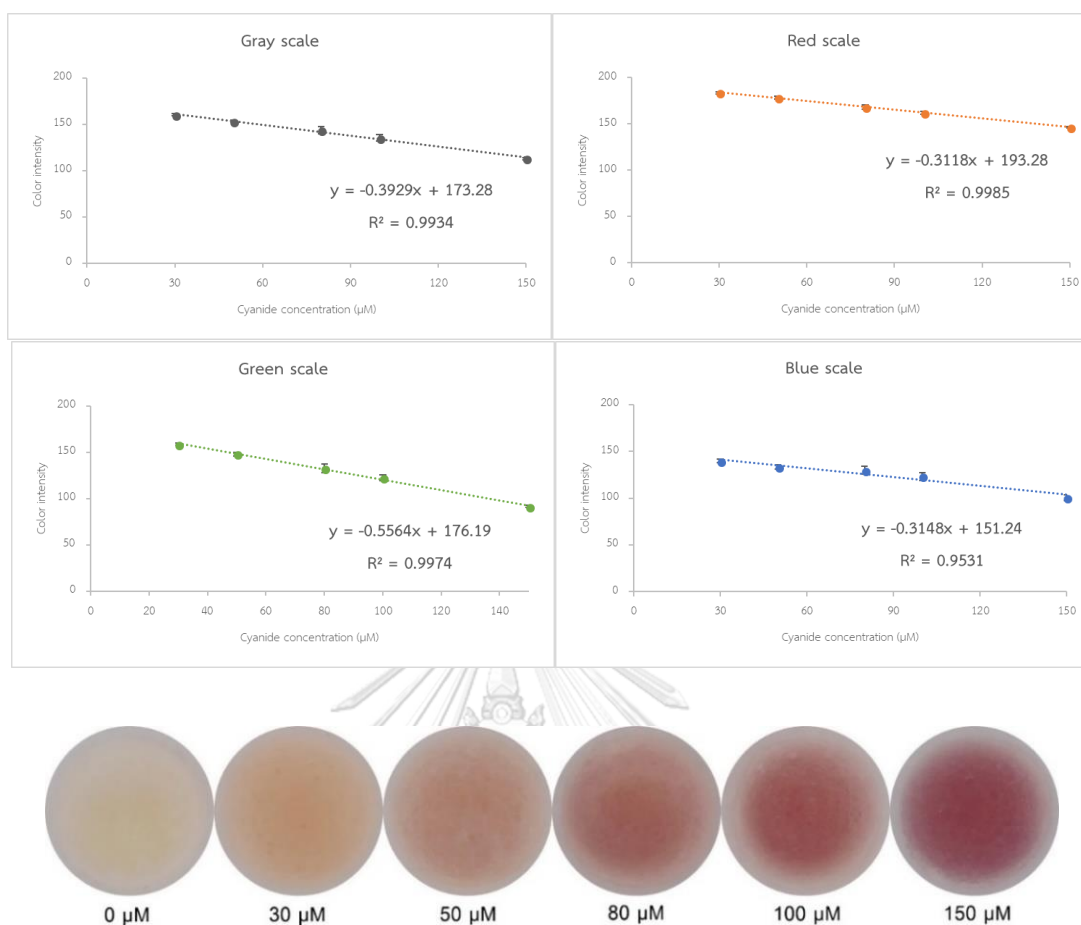


Figure 4.13 Calibration curve for cyanide determination using ferriin and CTAB-modified silica and material color chart.

4.3.2 Limit of detection

The limit of detection (LOD) of the proposed method was obtained from the analysis of blank solution by the proposed method. The experiment was performed followed section 3.5.1 under the optimum condition. The color intensity obtained at LOD concentration was calculated by the mean value μM acquired from blank solution analysis (I_{blk}) minus three times of standard deviation (SD_{blk}) ($n=10$). The LOD value of 17.20 μM was obtained while the LOD by naked eyes was 50 μM .

4.4 Effect of foreign ions

The effect of foreign ions that are often found in natural water or water samples was investigated. In this work, the detection of cyanide was performed in a binary mixture containing 50 or 100 μM cyanide and 1 mM foreign ion. This level of foreign ion was chosen according to the level of anions which are generally found in drinking water i.e. 250 ppm of chloride and sulfate reported by US EPA[59]. The color of materials observed and the color intensities are presented in Table 4.6 and Fig 4.14, respectively. The color of the materials used to detect high concentration of cyanide in the absence and in the presence of most foreign ions was similar. The results were confirmed by t-test that the color intensities were not significantly different at 95% confidence level (fluoride ($P=0.399$), chloride ($P=0.800$), bromide ($P=0.418$), iodide ($P=0.974$), iodate (0.052), and carbonate (0.439)). At low concentration of cyanide, the presence of 1 mM foreign ions strongly affected the detection given that the material color was paler, except for SCN. The results were confirmed by t-test. It was found that the color intensities of the materials used to detect 50 μM cyanide in the absence and in the presence of foreign ions were significantly different at 95% confidence level, except for the presence of iodide ($P= 0.950$).

The presence of iodate ions yielded very pale color especially at low concentration of cyanide. Iodate is an oxidizing agent that can oxidize Fe(II) in ferriin to Fe(III) lowering the amount of ferriin in the system and resulting a negative error.[60, 61] In addition, the presence of sulfate also gave negative result as Fe(II) can form complex with sulfate ions. On the other hand, the presence of thiocyanate ions resulted in more intense purple color on the material as thiocyanate can react with ferriin to yield $\text{Fe}(\text{phen})_3(\text{SCN})_2$ complex which is also purple.[58] This complex caused the positive error in cyanide detection.

Table 4.6 Effect of foreign ions on material color used to detect cyanide ions

CN ⁻ concentration (μM)	Anions								
	CN ⁻	CN ⁻ + F ⁻	CN ⁻ + Cl ⁻	CN ⁻ + Br ⁻	CN ⁻ + I ⁻	CN ⁻ + IO ₃ ⁻	CN ⁻ + HCO ₃ ⁻	CN ⁻ + SO ₄ ²⁻	CN ⁻ + SCN ⁻
50									
100									

(condition: 15 mg of CTAB-coated silica, 15 mL of sample volume, 5 mM CTAB added to sample mixture, 5 minutes of extraction time)

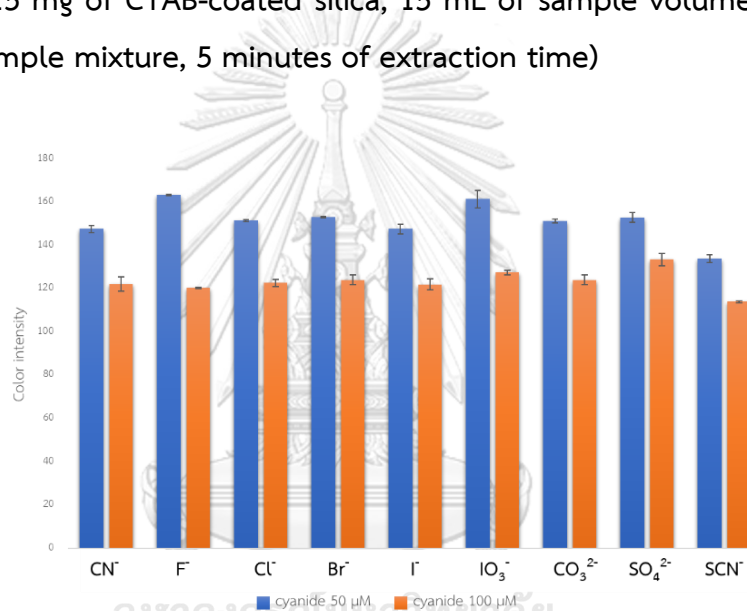


Figure 4.14 The color intensity observed in the detection of cyanide in standard solution in the absence (cyanide blank) and in the presence of various foreign ions (1 mM).

4.5 Determination of cyanide in water samples

Water samples were collected from several sources and analyzed by the proposed method (section 3.5.1) under the optimum condition.

4.5.1 Effect of water sample matrix

The effect of water sample matrix was examined by comparing the standard addition calibration curve of water sample with external standard calibration curve in the concentration range of 0-150 μM . The calibration curves are shown in Fig 4.15. The calibration curve in this section was plotted between cyanide concentration and delta color intensity (Δ intensity) that was calculated from the difference of color intensity of material color used in reagent blank solution and standard solution or spiked water sample. For the analysis of water sample, the most suitable color scale of image J was red scale due to different color tone of material obtained from standard and water sample.

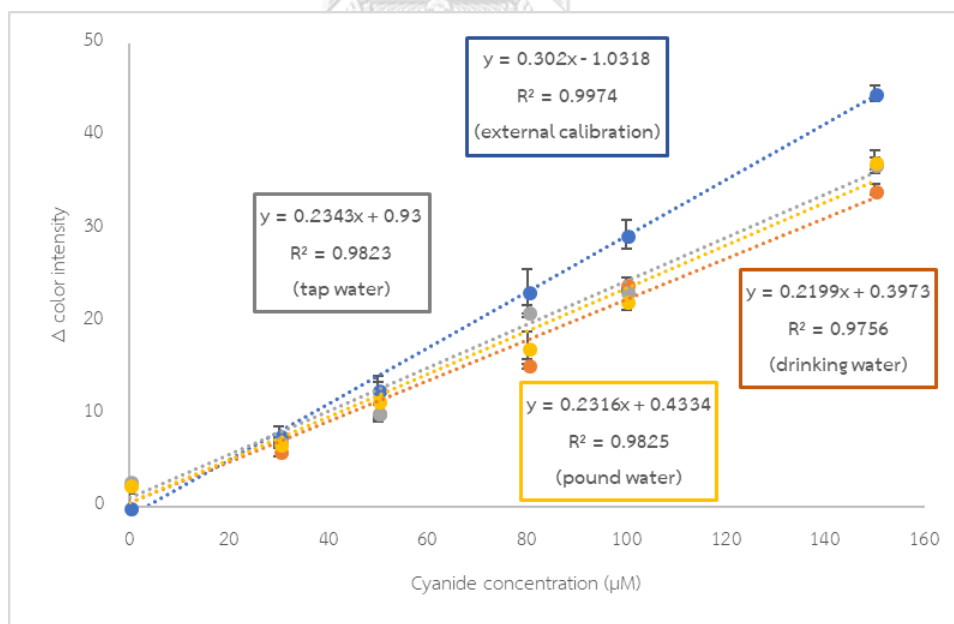


Figure 4.15 External calibration curve and standard addition calibration curve for determination of cyanide in water sample.

It was observed that the slope of external calibration curve and standard addition calibration curve of every water samples were different. The calibration curves of standard addition method had lower slope than that of the external calibration curve. It indicated that the matrix of water sample affected the determination and resulted in a lower sensitivity of cyanide detection. In addition, the color of materials used in water samples was obviously in different tone from the color observed in standard solution, in particular at low concentration of cyanide (Fig 4.16). The color of solids was in red-purple tone in standard solutions, while it had purple color in water samples. As shown in our previous study, other anions that can compete with cyanide in complex formation or reduce the amount of ferroin reagent would exhibit interference effect in the detection. Furthermore, the water sample matrix may differ from one sample to another; hence the standard addition method was applied for determining cyanide in water samples.

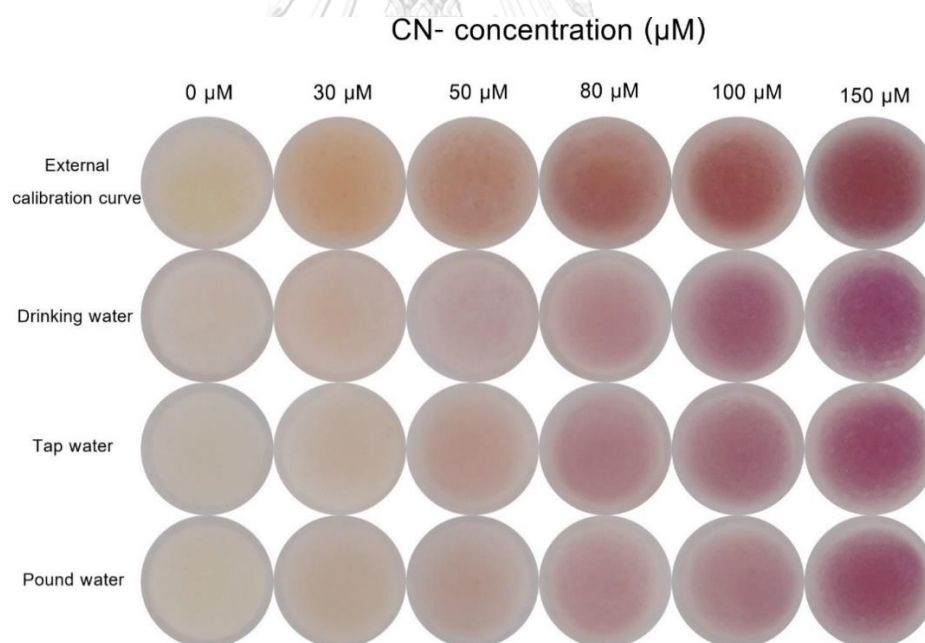


Figure 4.16 Color of materials used to detect cyanide in standard solution and in different spiked water samples.

4.5.2 Accuracy and precision in water sample analysis

To evaluate the accuracy of the method, the proposed method was applied to detect cyanide in water samples and the obtained results were compared to the results from using ion chromatography. Additionally, the samples spiked with known amount of cyanide were analyzed by both methods to evaluate the recovery of the analytes. Standard addition method was adopted to determine cyanide ion samples by the proposed method, while the external standard method was applied in the analysis by chromatography. The accuracy and precision of these methods are evaluated and presented in term of %recovery and %RSD, respectively. The results achieved from both methods are compared in Table 4.7.

The percent recovery obtained by the proposed method was in the range of 83.00 – 99.49 %, compared to 91.80 – 143.93 % by ion chromatography method. The relative standard deviation (%RSD) of the proposed method was found in the range of 1.23 – 7.14 %, compared to 1.00 – 10.39 % of ion chromatography method. These results indicate that the proposed method can be used to detect cyanide in water sample with acceptable accuracy and precision according to the criteria of AOAC international. [53]

Nevertheless, the results from ion chromatography was higher than those from the propose method for the analysis of every samples. The concentrations of cyanide in water samples determined by proposed method were significantly different from the values observed by ion chromatography method when compared by pair T-test at 95% confidence level, except for drinking water sample.

For drinking water, the results of both methods were not significantly different, indicated that the results from the proposed method were comparable to those from the instrument. Unfortunately, the results of tap water and pound water observed by the proposed method were significantly different from those of the instrument. In case of tap water, the %recovery obtained by ion chromatography method was higher than the acceptable level. The positive error results were probably caused by the contamination or the condition of instrument was not suitable for analysis cyanide

in this sample. For pond water, cyanide in non-spiked sample was found by instrument but not found by proposed method.

It should be taken in consideration that in ion chromatography, cyanate ions (CNO^-) if present in sample would also give the signal at the same retention time as cyanide. In ion chromatography, cyanide would be changed to cyanate when mixed with KOH eluent[38], hence the signal of the both species would occur at the same retention time. Consequently, the results of cyanide would be false positive if cyanate is present in sample and external standard calibration is used. On the other hand, in the proposed method, cyanate would not form complex with ferriin and the matrix problem was overcome by standard addition method.



Table 4.7 Determination of cyanide in water samples by the proposed method and ion chromatography method

Sample	Amount	Proposed method			Ion chromatography method		
	added	Found*	Recovery	RSD	Found*	Recovery	RSD
	(μM)	(μM)	(%)	(%)	(μM)	(%)	(%)
Drinking water	-	n.d.	-	-	n.d.	-	-
	30.00	29.09 \pm 2.08	97.00	7.14	32.98 \pm 1.18	109.93	3.57
	50.00	48.31 \pm 3.09	96.63	6.40	54.06 \pm 0.59	107.44	1.18
Tap water	-	n.d.	-	-	n.d.	-	-
	30.00	28.45 \pm 0.34	94.83	1.23	43.18 \pm 3.12	143.93	10.39
	50.00	41.50 \pm 1.02	83.00	2.45	58.82 \pm 0.59	117.64	1.00
Pond water	-	n.d.	-	-	56.10 \pm 1.02	-	-
	30.00	29.85 \pm 1.92	99.49	6.45	83.64 \pm 1.02	91.80	3.70
	50.00	43.44 \pm 2.34	86.88	5.38	103.7 \pm 1.56	95.20	3.27

*mean \pm SD (n=3), n.d. = non detectable

CHEAPTER V

CONCLUSION

5.1 Conclusion

In this research, a new simple and selective colorimetric method for cyanide determination was developed based on the complex formation of Tris-(1,10-phenanthroline) iron(II) with cyanide and the extraction of the dicyano-bis-(1,10-phenanthroline)-iron(ii) complex onto CTAB-coated silica. The change of material color from pale orange to purple related to cyanide concentration could be clearly observed by naked-eye. The optimal condition for cyanide determination was obtained by examining the effect of various parameters. The neutral dicyano-bis-(1,10-phenanthroline)-iron(ii) complex was formed in sample solution by using 15 mL of sample volume mixed with reagents to obtain the final concentration of 0.25 mM of ferroin and 5 mM of CTAB in the sample mixture. CTAB-coated silica could successfully extract the complex onto its surface with 5 minutes of extraction time. For the quantitative analysis, the color intensity was measured by image-J in RGB mode. Under the optimal condition, the linear working range of this method was 30 to 150 μM cyanide with a correlation coefficient (R^2) of 0.9974, and a limit of detection of 17.20 μM .

For study of the effect of foreign ions commonly found in water sample, most anions studied affected the analysis of low cyanide concentration. According to the matrix effect, the standard addition method was required for detecting cyanide in water sample. The percent recovery obtained by the proposed method was in the range of 83.00 – 99.49 %, compared to 91.80 – 143.93 % by ion chromatography method. The relative standard deviation (%RSD) of the results obtained was found in the range of 1.23-7.14%, compared to 1.00 – 10.39 % by ion chromatography method.

5.2 Suggestion for future work

Sample preparation should be applied to overcome the matrix effect in the determination cyanide in water sample. Moreover, this method could be used to detect cyanide in food sample such as cassava, almond or bamboo shoot after a proper sample preparation. The method sensitivity could be improved by preconcentration of cyanide by anion exchange resin before the detection with the proposed method. In addition, a column method and a flow system could also be applied to handle high sample volume in order to improve the detection sensitivity.



REFERENCES

- [1] U.S. Department of Health and Human Services Public Health Service. Toxicological Profile for Cyanide, Atlanta, Georgia: Agency for Toxic Substances and Disease Registry Division of Toxicology and Environmental Medicine/Applied Toxicology Branch, 2006.
- [2] Jones, L.H. Nature of Bonding in Metal Cyanide Complexes as Related to Intensity and Frequency of Infrared Absorption Spectra. Inorganic Chemistry 2(4) (1963): 777-780.
- [3] Lawson-Smith, P., Jansen, E.C., and Hyldegaard, O. Cyanide intoxication as part of smoke inhalation--a review on diagnosis and treatment from the emergency perspective. Scandinavian Journal of Trauma, Resuscitation and Emergency Medicine 19 (2011): 14.
- [4] Martin, T. Facts About Hydrogen Cyanide in Cigarette Smoke. 2017. Available from : <https://www.verywellmind.com/hydrogen-cyanide-in-cigarette-smoke-2824423> [2018, June 17]
- [5] Szilágyi, S. Banning Cyanide from Mining in the European Union. 1-13. Budapest: 2011.
- [6] Hopper, D.S.K. Small Animal Critical Care Medicine. 1st Edition ed. St. Louis, Missouri: Elsevier, 2008.
- [7] World Health Organization (WHO). Hydrogen Cyanide and Cyanides: Human Health Aspects, Geneva: World Health Organization, 2004.
- [8] European and National Drinking Water Quality Standards. European and National Drinking Water Quality Standards, Ireland, Northern Ireland: Environment Agency, 2011.
- [9] National Primary Drinking Water Regulations. In Ground Water and Drinking Water, United States Environmental Protection Agency. 2017.

- [10] Christison, T.T. and Rohrer, J.S. Direct determination of free cyanide in drinking water by ion chromatography with pulsed amperometric detection. Journal of Chromatography A 1155(1) (2007): 31-9.
- [11] Kameswara Rao, V., Suresh, S., Bhattacharya, A., and Rao, N.B.S.N. A potentiometric detector for hydrogen cyanide gas using silver dicyano complex. Talanta 49(2) (1999): 367-371.
- [12] Kaushik, R., Ghosh, A., Singh, A., Gupta, P., Mittal, A., and Jose, D.A. Selective Detection of Cyanide in Water and Biological Samples by an Off-the-Shelf Compound. ACS Sensors 1(10) (2016): 1265-1271.
- [13] Gholamzadeh, P., Mohammadi Ziarani, G., Lashgari, N., Badiei, A., Shayesteh, A., and Jafari, M. A Simple Colorimetric Chemosensor for Naked Eye Detection of Cyanide Ion. Journal of Fluorescence 26(5) (2016): 1857-64.
- [14] Cheng, C., Chen, H.-Y., Wu, C.-S., Meena, J.S., Simon, T., and Ko, F.-H. A highly sensitive and selective cyanide detection using a gold nanoparticle-based dual fluorescence–colorimetric sensor with a wide concentration range. Sensors and Actuators B: Chemical 227 (2016): 283-290.
- [15] Yang, Y., et al. Validation of an in vitro method for the determination of cyanide release from ferric-hexacyanoferrate: Prussian blue. Journal of Pharmaceutical and Biomedical Analysis 43(4) (2007): 1358-63.
- [16] Chaudhary, M.T., et al. Rapid and Economical Colorimetric Detection of Cyanide in Blood Using Vitamin B₁₂. Australian Journal of Forensic Sciences 48(1) (2016): 42-49.
- [17] Schilt, A. A., Colorimetric Determination of Cyanide Tris (1,10 Phenanthroline)-Iron(II) Ion as A Selective And Sensitive Reagent. Analytical Chemistry 30 (8) (1958): 1409-1411.
- [18] Zelder, F.H. Specific Colorimetric Detection of Cyanide Triggered by a Conformational Switch in Vitamin B₁₂. Inorganic Chemistry 47(4) (2008): 1264-1266.
- [19] Chaicham, A., Kulchat, S., Tumcharern, G., Tuntulani, T., and Tomapatnaget, B. Synthesis, photophysical properties, and cyanide detection in aqueous solution of BF₂-curcumin dyes. Tetrahedron 66(32) (2010): 6217-6223.

- [20] Männel-Croisé, C. and Zelder, F. Rapid visual detection of blood cyanide. Anal. Methods 4(9) (2012): 2632-2634.
- [21] Mannel-Croise, C. and Zelder, F. Complex samples cyanide detection with immobilized corrinoids. ACS Applied Materials & Interfaces 4(2) (2012): 725-9.
- [22] Tyrode, E., Rutland, M.W., and Bain, C.D. Adsorption of CTAB on Hydrophilic Silica Studied by Linear and Nonlinear Optical Spectroscopy. Journal of the American Chemical Society 130(51) (2008): 17434-17445.
- [23] Britannica, T. Cyanide. Encyclopaedia Britannica, Inc. 2018.
- [24] Simeonova, F.P. World Health Organization. Hydrogen cyanide and cyanides: Human health aspects, Geneva: 2004.
- [25] ATSDR. Medical Management Guidelines for Hydrogen Cyanide, Agency for toxic substances and disease registry. 2014.
- [26] Greaves, I. and Hunt, P. Chemical Agents. in Responding to Terrorism, pp. 233-344. Edinburgh: Churchill Livingstone, 2010.
- [27] David L. Nelson, M. M. C. Lehninger PRINCIPLES OF BIOCHEMISTRY. Freeman, W. H. & Company.
- [28] Dhas, P.K., Chitra, P., Jayakumar, S., and Mary, A.R. Study of the effects of hydrogen cyanide exposure in Cassava workers. Indian Journal of Occupational and Environmental Medicine 15(3) (2011): 133-136.
- [29] ATSDR. Toxicological Profile for Cyanide. in relevance to public health, Georgia: Atlanta, 13-23.
- [30] Parga, J.R., Valenzuela, J.L., Vazquez, V., Rodriguez, M., and Moreno, H. Removal of Aqueous Lead and Copper Ions by Using Natural Hydroxyapatite Powder and Sulphide Precipitation in Cyanidation Process. Materials Sciences and Applications 04(04) (2013): 231-237.
- [31] Bolarinwa, I.F., Oke, M.O., Olaniyan, S.A., and Ajala, A.S. A Review of Cyanogenic Glycosides in Edible Plants. (2016).
- [32] Boxer, G.E. and Rickards, J.C. Studies on the metabolism of the carbon of cyanide and thiocyanate. Archives of Biochemistry and Biophysics 39(1) (1952): 7-26.

- [33] What are EPA's drinking water regulations for cyanide [Online]. Available from: <https://safewater.zendesk.com/hc/en-us/articles/212077077-4-What-are-EPA-s-drinking-water-regulations-for-cyanide-> [2018, June 17]
- [34] Ma, J. and Dasgupta, P.K. Recent developments in cyanide detection: a review. Analytica Chimica Acta 673(2) (2010): 117-25.
- [35] Vallejo-Pecharromán, B. and Luque de Castro, M.D. Determination of cyanide by a pervaporation–UV photodissociation–potentiometric detection approach. The Analyst 127(2) (2002): 267-270.
- [36] Amayreh, M.Y. and Abulkibash, A.M. Differential Electrolytic Potentiometry: a Detector in the Flow Injection Analysis of Cyanide Using Silver Electrodes Modified with Carbon Nanotubes. Arabian Journal for Science and Engineering 42(10) (2017): 4445-4451.
- [37] Small, H. The evolution of modern ion chromatography. Reactive Polymers, Ion Exchangers, Sorbents 7(2) (1988): 73-80.
- [38] Destanoğlu, O., Gümüş Yılmaz, G., and Apak, R. Selective Determination of Free Cyanide in Environmental Water Matrices by Ion Chromatography with Suppressed Conductivity Detection. Journal of Liquid Chromatography & Related Technologies 38(16) (2015): 1537-1545.
- [39] Ding, M. and Wang, K. Determination of cyanide in bamboo shoots by microdiffusion combined with ion chromatography-pulsed amperometric detection. ROYAL SOCIETY OPEN SCIENCE 5(4) (2018): 172128.
- [40] Bhowmick, I., Boston, D.J., Higgins, R.F., Klug, C.M., Shores, M.P., and Gupta, T. Naked eye detection of cyanide in water with Co II bis(terpyridine) complexes. Sensors and Actuators B: Chemical 235 (2016): 325-329.
- [41] G-Biosciences, CTAB; Cat. # DG094; St Louis, MO, USA: G-Biosciences, 2016
- [42] Das, N., Cao, H., Kaiser, H., Warren, G.T., Gladden, J.R., and Sokol, P.E. Shape and size of highly concentrated micelles in CTAB/NaSal solutions by Small Angle Neutron Scattering (SANS). Langmuir 28(33) (2012): 11962-8.
- [43] Moon, S.Y., Kusunose, T., and Sekino, T. CTAB-Assisted Synthesis of Size- and Shape-Controlled Gold Nanoparticles in SDS Aqueous Solution. Materials Letters 63(23) (2009): 2038-2040.

- [44] Sizun, C., Raya, J., Intasiri, A., Boos, A., and Elbayed, K. Investigation of the surfactants in CTAB-templated mesoporous silica by ^1H HRMAS NMR. Microporous and Mesoporous Materials 66(1) (2003): 27-36.
- [45] Khoshnevisan, K., Barkhi, M., Zare, D., Davoodi, D., and Tabatabaei, M. Preparation and Characterization of CTAB-Coated Fe_3O_4 Nanoparticles. Synthesis and Reactivity in Inorganic, Metal-Organic, and Nano-Metal Chemistry 42(5) (2012): 644-648.
- [46] Wangchareansak, T., Keniry, M.A., Liu, G., and Craig, V.S. Coadsorption of low-molecular weight aromatic and aliphatic alcohols and acids with the cationic surfactant, CTAB, on silica surfaces. Langmuir 30(23) (2014): 6704-12.
- [47] Ma, X., Lee, N.H., Oh, H.J., Hwang, J.S., and Kim, S.J. Preparation and Characterization of Silica/Polyamide-imide Nanocomposite Thin Films. Nanoscale Research Letters 5(11) (2010): 1846-1851.
- [48] Woods, D.A., Petkov, J., and Bain, C.D. Surfactant adsorption kinetics by total internal reflection Raman spectroscopy. 2. CTAB and Triton X-100 mixtures on silica. The Journal of Physical Chemistry B 115(22) (2011): 7353-63.
- [49] Elias, S.D.; Rabiou, A. M.; Oluwaseun, O.; Seima, B. Adsorption Characteristics of Surfactants on Different Petroleum Reservoir Materials. The Online Journal of Science and Technology 6 (4) (2016): 6-16.
- [50] Huanca-Mamani, W., Rivera-Cabello, D., and Maita-Maita, J. A simple, fast, and inexpensive CTAB-PVP-silica based method for genomic DNA isolation from single, small insect larvae and pupae. Genetics and molecular research 14(3) (2015): 8001-7.
- [51] Ghosh, D., Pradhan, A.K., Mondal, S., Begum, N.A., and Mandal, D. Proton transfer reactions of 4'-chloro substituted 3-hydroxyflavone in solvents and aqueous micelle solutions. Physical Chemistry Chemical Physics 16(18) (2014): 8594-607.
- [52] Cantrell, K., Erenas, M. M., Orbe-Paya, I. de., and Capitán-Vallvey, L. F. Use of the Hue Parameter of the Hue, Saturation, Value Color Space As a Quantitative Analytical Parameter for Bitonal Optical Sensors. Analytical Chemistry 82 (2010): 531-542.

- [53] [AOAC Official Methods of Analysis, 2016 [Online]. Available from: http://www.aoac.org/aoac_prod_imis/AOAC_Member/ANews/2016_News/NEWS_021116.aspx [2018, June 10]
- [54] Table of Acids with Ka and pKa Values [Online]. 2018 Available from: <http://clas.sa.ucsb.edu/staff/Resource%20folder/Chem109ABC/Acid,%20Base%20Strength/Table%20of%20Acids%20w%20Kas%20and%20pKas.pdf> [2018, June 20]
- [55] Burgess, J. Kinetics of Reaction of Substituted Tris-(1,10-phenanthroline) iron(II) Complexes with Cyanide. Inorganica. Chimica. Acta. 5 (1) (1971): 133-136.
- [56] Chaudhuri, A., Haldar, S., and Chattopadhyay, A. Structural transition in micelles: novel insight into microenvironmental changes in polarity and dynamics. Chemistry and Physics of Lipids 165(4) (2012): 497-504.
- [57] G-Biosciences, CTAB; Cat. # DG094; St Louis, MO, USA: G-Biosciences, 2016
- [58] Ellingsworth, E.C., Turner, B., and Szulczewski, G. Thermal conversion of [Fe(phen)₃](SCN)₂ thin films into the spin crossover complex Fe(phen)₂(NCS)₂. RSC Advances 3(11) (2013): 3745.
- [59] United States Environmental Protection Agency (U.S. EPA). Drinking Water Contaminants: National Primary and Secondary Drinking Water Regulations Washington, DC, USA: U.S. EPA, 2009.
- [60] Ige, J.; Ojo, F.; Can, O. O. Kinetics and mechanism of oxidation of tris-(1,10-phenanthroline) iron(II) by chlorine and bromine and of the reduction of tris-(1,10-phenanthroline) iron(III) by iodide ions. Canadian Journal of Chemistry 57 (1979): 2065-2070.
- [61] Ali, I. H.; Eljack, N. D.; Sulfab, Y. Kinetics and Mechanism of Oxidation of Dicyanobis(bipyridyl)iron(II) by Periodate Ion in Aqueous Acidic Solutions. Journal of the American Chemical Society 3 (3) (2013): 68-76.



APPENDIX

จุฬาลงกรณ์มหาวิทยาลัย
CHULALONGKORN UNIVERSITY

VITA

Miss Patita Salee was born on August 7, 1992 in Bangkok Thailand. She received a Bachelor degree of Science from Chulalongkorn University in 2014. After that, she became a graduate student at the Department of Chemistry, Faculty of Science, Chulalongkorn University and a member of Environment Research and Unit under the supervision of Assistant Professor Dr. Fuangfa Unob. She completed Master's degree of Science in 2018.

